Michigan Institute for Plasma Science and Engineering (MIPSE)

17th ANNUAL GRADUATE STUDENT SYMPOSIUM

December 2, 2026
University of Michigan North Campus, Ann Arbor, MI 48109

Schedule

I. Special MIPSE Seminar

Johnson Rooms, 3213 Lurie Engineering Center, 1221 Beal Avenue

1:00 – 1:30 pm	**Registration, light lunch**
1:30 – 1:35 pm	**Prof. Mark J. Kushner**, University of Michigan Director, MIPSE ***Opening remarks***
1:35 – 2:45 pm	**Dr. Dave Ampleford,** Sandia National Laboratories ***The ZX Initiative - Expanding the Physics Capabilities of the Z Pulsed Power Facility***

II. Poster Presentations

Atrium
EECS Building, 1301 Beal Avenue

2:45 – 3:15 pm	Poster setup
3:15 – 4:00 pm	**Poster Session I**
4:00 – 4:45 pm	**Poster Session II**
4:45 – 5:30 pm	**Poster Session III**
5:30 – 5:45 pm	Poster removal
5:45 – 6:00 pm	***Best Presentation Award* ceremony**

Participating institutions: University of Michigan, Michigan State University.

Poster Session I

1-01	**Lucas Babati**	U-M	***Conductivity from the Spitzer Limit through Warm Dense Matter***
1-02	**Declan Brick**	U-M	***Regression Analysis of a Self-Consistent Anomalous Transport Closure in a Multi-Fluid Hall Thruster Model***
1-03	**Gonçalo Cardoso**	U-M	***Characterizing Directionality, Energy and Spatial Uniformity of Neutral Beams for Material Processing***
1-04	**Jesus Diaz Alcala**	U-M	***A Comparison of Hydrodynamic Enhancement and Surfactant Addition for PFAS Treatment***
1-05	**Ian Freeman**	MSU	***Modeling Radiatively Cooled Pulsed Power Reconnection Experiments Using the Open Source AthenaPK***
1-06	**Myles Gong**	U-M	***Impact of Discharge Current on the Response of Hall Effect Thrusters to Background Neutral Pressure***
1-07	**Jiashu Han**	U-M	***A Semi-Lagrangian Particle Method for the 1D1V Two-Species Vlasov–Poisson System and 2D Incompressible MHD in Vorticity–Current Form***
1-08	**Ishan Kanade**	U-M	***Geometry-Aware AMR for 2D FLASH Simulations of Capsule Implosions***
1-09	**Kyle Kemmerer**	U-M	***Molecular Dynamics Simulations of Magnetic-Field-Dependent Parallel Electrical Conductivity in Strongly Magnetized Plasmas***
1-10	**Adam Rouzky**	U-M	***Magnetic Flux Compression and Instability Growth in Argon Gas Puff Z Pinches onto a Solid Rod***
1-11	**Alex Timoney**	U-M	***Shock Density Analysis for Magnetized Collisionless Shocks on the Z Machine***
1-12	**Bingqing Wang**	U-M	***Kinetic Investigation of the Effects of Emission Mechanisms on Inverse Sheath Formation***
1-13	**Yeon Geun Yook**	U-M	***Circuit-Induced Transients and Ion Energy Control in Pulsed-Bias Capacitively Coupled Plasmas***
1-14	**Grace Zoppi**	U-M	***Experimental Characterization of a Co-Axial Electrodeless Magnetoplasmadynamic Thruster***
1-15	**Jisu Jeon**	U-M	***PFOA Degradation in Water: Long-Time-Scale Modeling Investigation***
1-16	**Katie Ballard**	U-M	***An Investigation of Extreme Low-Density and Low-Speed Solar Wind***
1-17	**Shane Keiser**	U-M	***Micropinch Characterization on Hybrid X-pinches using the PERSEUS xMHD Code***
1-18	**Corey Gui**	U-M	***On the Evolution of the Magneto-Rayleigh Taylor Instability in Cylindrical Geometry***

Poster Session II

2-01	**Victoria Collemi**	U-M	***Effect of Orbital Angular Momentum on Wake Instabilities in a Laser Wakefield Accelerated Beam***
2-02	**Carter Krumins**	U-M	***Investigation of Oxygen Resilience of Thermionic Emitters for Electric Propulsion***
2-03	**Chenyao Huang**	U-M	***Dynamics of Charge Conduction in Water Layers Formed During Cryogenic Etching of HAR SiO_2 Features***
2-04	**Alexander Loomis**	MSU	***Chemical Vapor Deposition of Delta-Doped Diamond with a NIRIM Type Reactor***
2-05	**Md Arifuzzaman Faisal**	U-M	***Current Crowding and Contact Resistance in Anisotropic 2D Devices***
2-06	**Adam Brusstar**	U-M	***Simulation and Experimental Demonstration of an Overmoded X-band Magnetically Insulated Line Oscillator***
2-07	**Sarah Feldman**	U-M	***HEROICS: A SWaP-Efficient Triple Coincidence Time of Flight Plasma Spectrometer***
2-08	**Josh Fung**	U-M	***Modeling the Longitudinal Dependence of Radiation Belt Electron Dynamics at Earth and Jupiter***
2-09	**Julian Kinney**	U-M	***Nuclear Fusion Enhancement in Dense Plasmas***
2-10	**Wanglim Song**	U-M	***Two-dimensional Quantum-Mechanical Analysis of Ion-Enhanced Thermionic and Thermo-Field Emission and the Peak-Current Phenomenon***
2-11	**James Welch**	U-M	***Simulations and Experiments Measuring Temperature Relaxation Rates in a Strongly Magnetized Antiproton-Electron Plasma***
2-12	**Ari Eckhaus**	U-M	***Effects of Back Wall Material in an ECR Magnetic Nozzle Thruster***
2-13	**Marissa Knofczynski**	U-M	***Diagnostic Development of X-pinch Backlighters on the MAIZE Pulsed Power Facility***
2-14	**Kwyntero Kelso**	U-M	***X-ray Absorption Spectroscopy Experiments of Radiatively Ionized Argon Gas***
2-15	**Emily Hong**	U-M	***Effects of Elevated Concentrations of Ammonia and Hydrogen Sulfide on Non-Thermal Plasma Inactivation of Airborne Viruses***
2-16	**Braden Oh**	U-M	***Electrostatic-Magnetic Retardation of a Low-Temperature Ion Beam for Backsputter Mitigation***
2-17	**Codie Fiedler Kawaguchi**	U-M	***Identifying Informative Designs for Constraining Rheological Properties under Shocked Conditions***
2-18	**Nicholas Donatelli**	U-M	***Phase-Resolved Optical Emission Spectroscopy of Kr/Water Mixtures in a Pulsed 13.6 MHz RF ICP***

Poster Session III

3-01	**John Riley O'Toole**	U-M	***Comparison of Laser Thomson Scattering and Langmuir Probe Near-Field Electron Measurements on a 9 kW Hall Effect Thruster***
3-02	**Yves Heri**	U-M	***Relativistic Electron Beam Transport and Pulse Broadening in a Diode–Drift System***
3-03	**Jarett LeVan**	U-M	***Extending Plasma Kinetic Theory: Memory, Magnetic Fields, and Strong Coupling***
3-04	**William Maxon**	U-M	***Novel Quasi-Analytic Solutions of Radiation Diffusion in Heterogeneous Media***
3-05	**Alejandro Padilla Gomez**	MSU	***Quantum-Correct Bhatnagar-Gross-Krook Operator for Coupling Collisions to the Wigner-Poisson Model***
3-06	**Nolan Tribu**	U-M	***Determining Energy Flux Across the Dayside Magnetopause Induced by Boundary Motion***
3-07	**Nathaniel Bowers**	U-M	***Development and Characterization of an Al Vapor Target for Ionization Front Experiments***
3-08	**Michelle Bui**	U-M	***DMSP SSUSI & SSJ Auroral Oval Model Validation***
3-09	**Briggs Damman**	U-M	***Calculating the Thermal Conductivity of a Two-Component Plasma Using Non-equilibrium Molecular Dynamics Simulations***
3-10	**Filomela V. Gerou**	U-M	***Platform for X-Pinch Radiography Capability of Shock Propagation Through a Foam***
3-11	**Yifan Gui**	U-M	***Tailored Voltage Waveforms in Inductively Coupled Plasmas for Cryogenic Etching using Ar/HF Gas Mixtures***
3-12	**Lan Jin**	U-M	***Effect of Temporal Optical Pulse Asymmetry on Ultrafast Photoemission***
3-13	**Miron Liu**	U-M	***Spatial Anti-aliasing Optical Plasma Wave Diagnostics for Low Temperature Plasma Sources***
3-14	**Jeremy Rebenstock**	U-M	***High-energy Narrow-divergence Electron Beam Generation from High Intensity Solid Target Interactions using the ZEUS Laser System***
3-15	**Tianqi Sun**	U-M	***Intrinsic Mean Transverse Energy in Electron Emission Across Multiple Emission Regimes***
3-16	**Tetiana Tymoshevska**	U-M	***Conceptual Design of an Electrospray-Enabled Liquid Droplet Radiator***
3-17	**Xinyan Xiang**	U-M	***Coherent Spectroscopy of Rydberg Levels in Discharge Plasma for Electric Field Sensing***
3-18	**Moises Enriquez**	U-M	***Kinetic-informed Fluid Model for Cross-field Sheaths in Multi-ion Species Plasmas***

Abstracts: Poster Session I

Conductivity from the Spitzer Limit through Warm Dense Matter*

Lucas J. Babati[a], Nathaniel R. Shaffer[b], Louis Jose[a] and Scott D. Baalrud[a]

(a) Nuclear Engineering and Radiological Sciences, University of Michigan, Ann Arbor, MI
(b) Laboratory for Laser Energetics, Rochester NY

A theoretical model is developed to compute electronic transport coefficients extending from warm and dense to hot and dilute plasma conditions. The approach is based in kinetic theory and models strong Coulomb correlations by treating binary interactions using the potential of mean force, electron degeneracy using the Uehling-Uhlenbeck equation, and diffraction using quantum mechanical cross sections. This treatment allows the model to extend from the weakly coupled plasma regime through the warm dense matter regime where typical plasma theories would break down. The model provides an accurate means to compute electrical conductivity, thermal conductivity, and electrothermal coefficients, while including contributions from electron-electron collisions. This is an effect which is not present in most calculations of conductivities in the warm dense matter regime and is shown to be a significant factor when included. A comparison between the present model and other theories as well as experiments is made for solid density aluminum showing excellent agreement. Further, agreement is shown to density functional theory molecular dynamics (DFT-MD) in warm dense hydrogen when electron-electron collisions are not included. When they are included, a correction of over a factor of two can be incurred. Finally, this model is computationally efficient in comparison to DFT-MD, which allows for the rapid production of tables of coefficients necessary to model inertial confinement fusion, stellar evolution, and high energy density plasma experiments.

* This work is funded by the U.S. Department of Energy NNSA Center of Excellence under cooperative Agreement No. DE-NA0004146 and by the Department of Energy [National Nuclear Security Administration] University of Rochester “National Inertial Confinement Fusion Program” under Award Number DE-NA0004144.

Regression Analysis of a Self-Consistent Anomalous Transport Closure in a Multi-Fluid Hall Thruster Model*

Declan Brick and Benjamin Jorns

Department of Aerospace Engineering, University of Michigan (brickd@umich.edu)

Predictive engineering models of Hall thrusters have been hampered to date by the existence of anomalous electron transport. This process, which is fundamentally kinetic in nature, enhances the transport of electrons across field lines by orders of magnitude above the level that can be accounted for by classical effects. To rectify this problem, models of Hall thrusters often introduce an anomalous collision frequency in the system of electron equations to match experimental trends. However, the addition of this term introduces a closure problem as we now have more unknowns than equations. This issue has motivated the search for closures that express the anomalous collision frequency in terms of other plasma properties. Multiple decades of effort have been expended in allowing these closures to be predictive. One common feature across all closures are ad-hoc coefficients that are typically tailored to match experimental measurements. These coefficients represent physical constants or factors that arise out of phase-space averaging of the kinetic transport effects, so cannot be self-consistently captured in a fluid model. For a model to be predictive, it is therefore critical to understand how these coefficients vary with thruster operation and the range of coefficients that produce accurate descriptions of experimental data.

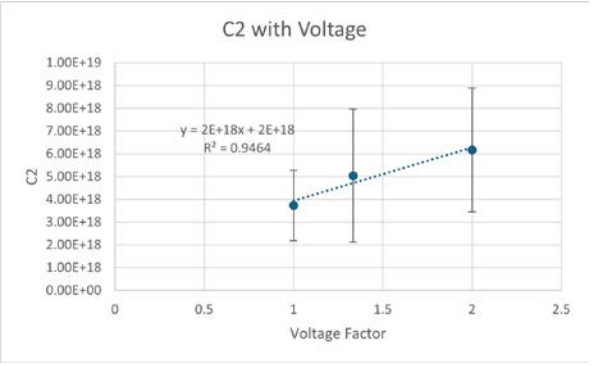


Figure 1 – Example of coefficient trendline with operating voltage. Points correspond to best fit parameters as determined by the GPR surrogate. Error bars correspond to the standard deviation of all C2 values within GPR error of the optimal parameters.

In this work we employ an anomalous collision frequency of the form:

$$\nu_{an} = c_1 \nu_{iz} + \frac{c_2}{n_n^{1.0} T_e^{1.5}}, \qquad \vec{E} \cdot \vec{j}_e = c_\Omega \vec{E} \cdot \vec{j}_e$$

Where ν_{an} is the anomalous collision frequency, c_1; c_2; and c_Ω are tunable constants, ν_{iz} is the ionization frequency, T_e is electron temperature, n_n is neutral density, $\vec{E}$ is the electric field, and $\vec{j}_e$ is the electron current density. We sample the three-dimensional parameter space for multiple operating conditions that vary the propellant, discharge current, and discharge voltage. Using Gaussian Process Regression (GPR), we fit a surrogate to the entire parameter space. With this surrogate we can identify the optimal set of parameters and the region of parameter space that agrees within GPR error to the best case parameters. By doing so, we are able to understand the trends of the coefficients with operating condition, as well as the error in the optimal values. We discuss the physical implications of these results in the context of developing predictive closure models for Hall thrusters.

* Work supported by an NSF GRFP, the NASA JANUS institute (80NSSC21K1118), DOE grant DE-SC0022988, and in part through computational resources and services provided by Advanced Research Computing at the University of Michigan.

Characterizing Directionality, Energy and Spatial Uniformity of Neutral Beams for Material Processing*

Gonçalo A. Cardoso[a] and Mark J. Kushner

(a) University of Michigan, Nuclear Engineering & Radiological Sciences Dept., Ann Arbor, MI 48109-2122, USA (gcardoso@umich.edu)

(b) University of Michigan, Electrical and Computer Engineering Dept., Ann Arbor, MI 48109-2122, USA (mjkush@umich.edu)

Ion bombardment onto biased wafers during plasma etching can result in charge buildup within features that can deflect incoming ion trajectories, resulting in feature defects such as bowing or notching, or lead to device damage. UV photons emitted from the plasma might also cause surface defects such as dangling bonds [1]. These issues are exacerbated as device dimensions are scaled down, due to larger electric fields for a given charging potential and increased surface-to-volume ratio. This is particularly the case for the fabrication of 2-dimensional materials consisting of nearly monolayer thickness. Energetic neutral beams have been proposed as an alternative, low-damage and charge-free technique for etching and deposition, and particularly so for 2D materials. Such beams can be produced through ion acceleration and subsequent neutralization, either through charge-exchange collisions (volume neutralization) or by reflection from surfaces (surface neutralization) [2, 3]. The primary technical challenges for neutral beam sources involve optimization of directionality, energy and spatial uniformity of the energetic neutral fluxes striking the substrate.

In this paper, we discuss the results of a computational investigation of a neutral beam source consisting of an inductively coupled plasma separated from the wafer by a radio frequency (RF) biased grid powered at 10 MHz. Typical conditions for this source are pressures of tens of mTorr, gas mixtures containing Ar, O2 and Cl2 and biases on the grid of hundreds of volts. This source has been simulated using the Hybrid Plasma Equipment Model (HPEM). The Plasma Chemistry Monte Carlo Module (PCMCM) in the HPEM tracks the motion of ions (and neutrals) as they are accelerated by electric fields, collide with background gas particles and neutralize by reflecting from the grid. The PCMCM records the resulting neutral energy and angular distributions (NEADs) at the wafer. This work investigates the characteristics of these NEADs at and how they are influenced by grid surface roughness (non-specular scattering), inelastic scattering from the grid, gas-phase charge-exchange reactions and pressure gradients across the grid.

*This work was supported by the US Department of Energy, Office of Science, Fusion Energy Sciences (FES) and Basic Energy Sciences (BES) as part of the Extreme Lithography & Materials Innovation Center (ELMIC), a Microelectronics Science Research Center (MSRC), through the Plasma-enabled 2D Materials project (DEAC02-09CH11466); and by FES (SC-00274510).

References

[1] S. Samukawa, ECS J. Solid State Sci. Technol. 4 (2015) N5089.
[2] S. Samukawa et al, Jpn. J. Appl. Phys. 40 (2001) L779.
[3] D.J. Economou, J. Phys. D:Appl. Phys. 41 (2008) 024001.

A Comparison of Hydrodynamic Enhancement and Surfactant Addition for PFAS Treatment*

Jesus Diaz Alcala, Alicia Dai, Sean Dickason, Aung Htoo Htet, Grace Herrin and John Foster

Nuclear Engineering & Radiological Sciences, University of Michigan (diazalc@umich.edu)

Per- and polyfluoroalkyl substances (PFAS) are a class of persistent anthropogenic chemicals characterized by highly stable carbon-fluorine bonds [1]. Their persistence to natural degradation has raised concerns about their accumulation in the environment and potential health effects for all. Plasma treatment is being investigated as a promising degradation strategy [2].

Many laboratory-scale plasma reactors for PFAS treatment rely on the transport of plasma-generated reactive species, ions, and electrons to the liquid phase to promote degradation. Unfortunately, the treatment of short-chain PFAS remains a challenge, as these species possess relatively low surface activity and a reduced tendency to accumulate at the plasma-liquid interface [3], which can limit exposure to and treatment by the plasma. Addition of surfactant has been explored to enhance transport to the interface [4], while hydrodynamic enhancement, such as turbulent mixing at the interface, may offer an alternative approach to improving treatment efficiency [5].

Presented here is a reactor that features high-speed recirculation to affect turbulent mixing at the plasma-liquid interface. The solution is forced through a shower head-like element, where water jets are produced with a high surface-to-volume ratio and are exposed to the plasma. With mixing and interfacial renewal, this approach may improve PFAS treatment without requiring additional surfactants.

This work investigates the relative effects of surfactant addition and solution recirculation rate on plasma treatment of PFAS. Experiments will compare treatment performance across different recirculation rates to vary interfacial turbulence and surfactant conditions, including their combined effects. Fluoride yield, conductivity, pH, plasma power consumption, hydrogen peroxide concentration, and PFAS degradation intermediates will be measured and monitored over time. These measurements will be used to evaluate the effects of hydrodynamic conditions and surfactant addition on PFAS degradation and fluoride production.

*This work was supported by NSF ECLIPSE #2512119 and the Anthropocene Institute.

References

[1] S. E. Fenton et al., Environ. Toxicol. Chem. 40, 606 (2021)
[2] C. A. Aggelopoulos, Sep. Purif. Technol. 380, 135535 (2026)
[3] Y.-J. Lee et al., npj Clean Water 9, 35 (2026).
[4] R. Li et al., Chem. Eng. J. 547, 180924 (2026)
[5] R. Klymenko et al., Plasma Sources Sci. Technol. 33, 045012 (2024).

Modeling Radiatively Cooled Pulsed Power Reconnection Experiments Using the Open Source AthenaPK*

Ian Freeman and Brian W. O'Shea

Michigan State University (freem386@msu.edu)

Magnetic reconnection, the explosive reorientation of magnetic field lines in current sheets, is an important and challenging computational problem in plasma physics. In high energy density environments, like those found in pulsed power experiments, the problem is numerically stiff, making MHD simulations computationally expensive. GPUs offer a shorter time-to-answer solution to this challenge than traditional CPU calculations. This work presents simulations of magnetic reconnection in pulsed power experiments inspired by the Magnetic Reconnection on Z (MARZ) experiments using the GPU-capable open-source codebase AthenaPK. We demonstrate the capabilities of AthenaPK to solve this problem and the enhanced reconnection rates produced by radiative cooling in pulsed power reconnection sheets. We also discuss necessary inclusions of temperature dependent resistivity and coupled iterative solvers to address numerical stiffness. We compare the formation of the current sheet under radiative cooling to recent analytical models and demonstrate that our simulations produce reconnection rates and dynamics predicted by modified Sweet-Parker reconnection rates.

*This material is based upon work supported by the National Science Foundation Graduate Research Fellowship Program under Grant No 2235783. This work is also supported in part by the National Science Foundation Research Traineeship Program (DGE-2152014) to Ian Freeman. Any opinions, findings, and conclusions or recommendations expressed in this material are those of the author(s) and do not necessarily reflect the views of the National Science Foundation.

References

[1] E. N. Parker, Astrophys. J. Suppl. Ser. 8, 177 (1963)
[2] D. A. Uzdenskyand J. C. McKinney, Phys. Plasmas 18, 042105 (2011)
[3] N. Loureiro, A. Schekochihin, and S. Cowley, Phys. Plasmas 14, 100703 (2007)
[4] R. Datta, et al., Phys. Plasmas 31, 052110 (2024)
[5] R. Datta, et al., Phys. Rev. Lett. (2024)132, 155102 (2024)
[6] R.Samtaney,etal.Phys. Rev. Lett. 103, 105004 (2009)

Impact of Discharge Current on the Response of Hall Effect Thrusters to Background Neutral Pressure

Myles Y. Gong, William J. Hurley and Benjamin A. Jorns

Department of Aerospace Engineering, University of Michigan
Ann Arbor Michigan, 48109

Increasing the discharge current to Hall thrusters offers a promising pathway to scaling electric propulsion systems to higher powers for space exploration, but reliable interpretation of ground-based performance measurements of these high-power devices requires careful consideration of vacuum-facility effects. It is a well-known effect that elevated background pressure can entrain additional neutrals into the discharge and modify ionization, acceleration, and plume characteristics, thereby affecting measured thrust and efficiency.[1]

Previous work has suggested that a critical metric driving the response of the thruster to facility pressure is not the absolute magnitude of facility pressure but rather the ratio of background neutrals to the density of neutrals emerging from the thruster.[2] This may suggest that thrusters with higher flow rates of neutrals may be less sensitive to facility effects.

To investigate this possibility, this study presents a parametric comparison of a krypton Hall thruster's performance, efficiency, and stability as a function of discharge current as measured in two separate facilities with an order of magnitude difference in background pressure. At lower discharge current operating conditions, it is found that the measured performance differences between facilities are large (> 20%), indicating high sensitivity to background pressure. As discharge current increases, differences in mass flow rate and thrust between facilities asymptotes to less than 10%. These results highlight the capacity of increased discharge current to partially mitigate facility-pressure effects. Several physical mechanisms are considered to explain this trend, including shifts in the acceleration region within the discharge channel as well as progressive changes in the mass utilization and beam utilization efficiencies with increasing discharge current.

References

[1] A. Piragino et al., Aerospace **8**, 69 (2021).
[2] N. MacDonald-Tenenbaum et al., Journal of Propulsion and Power **35**, 403–412 (2019).

A Semi-Lagrangian Particle Method for the 1D1V Two-Species Vlasov–Poisson System and 2D Incompressible MHD in Vorticity–Current Form

Jiashu Han[a], Robert Krasny[b] and Alexander Thomas[c]

(a) Department of Mathematics, University of Michigan (shujhan@umich.edu)
(b) Department of Mathematics, University of Michigan (krasny@umich.edu)
(c) Department of Nuclear Engineering and Radiological Sciences, University of Michigan (agrt@umich.edu)

We present a semi-Lagrangian particle method for two plasma models, one kinetic and one fluid. First, we solve the 1D1V two-species Vlasov–Poisson system, representing the electron and ion distribution functions on adaptively refined panels organized in a quadtree structure, with a 3×3 particle grid per panel. The electric field is computed by convolving the charge density with a regularized kernel, and the discrete N-body sums are evaluated with a GPU-accelerated treecode. The method is applied to ion acoustic waves, where we study long-time dynamics. Second, we extend the framework to 2D incompressible magnetohydrodynamics using a vorticity–current formulation, in which particles carry vorticity and current density, and the velocity and magnetic fields are recovered by Biot–Savart integrals with regularized kernels. The solver is verified on standard benchmarks including the Orszag–Tang vortex and applied to current-sheet dynamics relevant to plasmoid-mediated reconnection at high Lundquist number.

Geometry-Aware AMR and R_{NLTE} Tracking for 2D FLASH Simulations of Capsule Implosions*

Ishan Kanade[a], Heath LeFevre[a] Matthew Trantham[a], Julian Kinney[a],Scott Baalrud[a],Carolyn Kuranz[a] and Ryan McClarren[b]

(a) University of Michigan
(b) University of Notre Dame

Dense, strongly coupled, radiative plasma conditions in neutron star envelopes make them difficult to observe directly. Laser-driven capsule implosions provide a way to study this regime in a laboratory environment. We conduct simulations of these implosions with the FLASH code in 2D, extending previous 1D simulations. Simulated targets consist of micron-scale Ni and Al layers within a low-density chamber gas. Resolving these layers requires nanometer-scale cells, where the hydrodynamic CFL condition limits the time step so uniform refinement is computationally prohibitive. To allow for feasible simulations, we implement a geometry-aware AMR scheme tracking the evolving material layers, which focuses resolution near the laser-driven capsule instead of refining the full domain. We quantify mesh evolution and computational cost with leaf-block counts and runtime metrics. To identify shock propagation regions where LTE assumptions may break down, we process FLASH data using R_{NLTE}, defined as the ratio of photon mean free path to electron-temperature gradient scale length. We calculate photon mean free paths from LANL TOPS Rosseland opacities and FLASH material tracers. Spatial maps and cylindrical-volume-weighted averages of R_{NLTE} track NLTE-prone regions during the implosion.

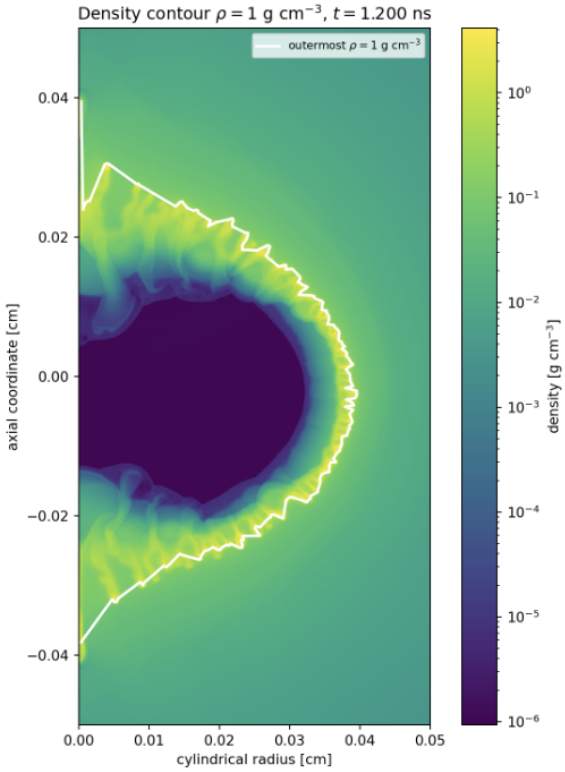


Figure 1: 2D FLASH simulation density profile at t = 1.200 ns illustrating spatial density distribution and the outermost tracked boundary contour during capsule implosion.

*Work supported by the NNSA Stockpile Stewardship Academic Alliances under grant number DE-NA0004100.

References

[1] B. Fryxell et al., "FLASH: An Architecture for Multiphysics Simulation," Astrophys. J. Suppl. Ser. **131, 273** (2000).
[2] N. H. Magee et al., "Atomic Structure Calculations and Opacity Tables," ASP Conf. Ser. **78, 51** (1995).
[3] J. J. MacFarlane et al., "Simulation of Radiation-Hydrodynamics and Non-LTE Physics in HEDP Experiments," High Energy Density Phys. 3, **181** (2007).

Molecular Dynamics Simulations of Magnetic-Field-Dependent Parallel Electrical Conductivity in Strongly Magnetized Plasmas*

Kyle Kemmerer, Louis Jose and Scott D. Baalrud

Department of Nuclear Engineering & Radiological Sciences, University of Michigan, Ann Arbor, MI
(kylekem@umich.edu)

Electrical conductivity parallel to the magnetic field governs how heat and current flow in strongly magnetized plasmas, from Z-pinch experiments and magnetized dusty plasmas to neutron star atmospheres and antimatter traps. In these strongly magnetized systems, the field is strong enough that the electron gyroradius drops below the Debye length ($\beta_e = \lambda_{De}/r_{ce} > 1$), fundamentally altering the trajectories of colliding particles [1].

Traditional kinetic theories assume that the magnetic field does not affect binary collisions, thereby predicting a parallel conductivity that is independent of field strength. However, a recent kinetic theory that retains the Lorentz force during collisions instead predicts that once $\beta_e > 1$, parallel conductivity rises with increasing magnetization and ultimately scales linearly with β_e [2].

To test this, molecular dynamics (MD) simulations of electrons and ions were run in LAMMPS, imposing an external electric field and measuring the induced current to extract the conductivity across a range of magnetization strengths and Coulomb coupling parameters. In the weakly magnetized limit, our results reproduce the classical field-independent values. At the onset of strong magnetization, however, the parallel conductivity rises as anticipated with β_e, confirming the predicted enhancement and providing a first-principles benchmark of the new theory.

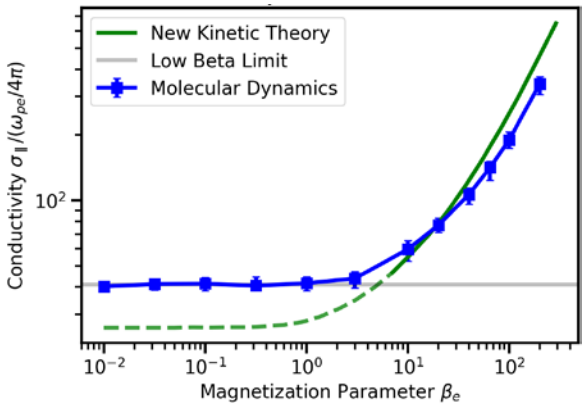


Figure 1 – Molecular dynamics simulation results (blue) for plasma conductivity parallel to the magnetic field as a function of magnetization parameter, alongside the predictions of a new kinetic theory that retains the Lorentz force during collisions (green). The MD data agrees with the classical field-independent predictions at low beta, before beginning to rise sharply at the onset of strong magnetization, showing good agreement with the new theory.

*This material is based upon work supported by NSF Grant Award No. PHY-2512424

References

[1] S. D. Baalrud and J. Daligault, Physical Review E **96**, 043202 (2017).
[2] L. Jose and S. D. Baalrud, Physics of Plasmas **27**, 112101 (2020).

Magnetic Flux Compression and Instability Growth in Argon Gas Puff Z-Pinches onto a Solid Rod

Adam Rouzky and Ryan McBride

University of Michigan (arouzky@umich.edu, mcbrider@umich.edu)

During high-power Z-pinch implosions, such as those performed in magnetized liner inertial fusion (MagLIF) on the Z-machine at Sandia National Laboratories, low-density electrode plasmas form in the power feed. These low-density plasmas are driven onto the outer surface of the dense liner target, where they can imprint structure and seed implosion instabilities. Experiments on the MAIZE facility at the University of Michigan have been performed to investigate the behavior of low-density plasmas imploding onto dense targets.[1,2] In these experiments, an annular gas puff z-pinch was used to emulate the low-density power feed plasma and a solid on-axis rod was used to emulate the dense liner. Recently, we have used the 3D Hall-magnetohydrodynamics code PERSEUS to model and simulate these experiments. The results of this computational effort are the subject of this presentation.

References

[1] J. M. Chen et al., IEEE Trans. Plasma Sci. **52**, 4876 (2024).
[2] J. M. Chen, PhD Dissertation, University of Michigan (2025).

Shock Density Analysis for Magnetized Collisionless Shocks on the Z Machine*

A. Timoney [a], D. Schneidinger [b], T. Van Hoomissen [b], H. Hasson [c], D. Yager-Elorriga[c], A. Sarracino [c], D. Schaeffer [b] and C. Kuranz [a]

(a) University of Michigan
(b) UCLA
(c) Sandia National Laboratories

Magnetized collisionless shocks are ubiquitous in heliospheric and astrophysical environments, including planetary bow shocks, the heliopause, supernova remnants, and galaxy clusters. Of particular interest are particle heating and non-stationary dynamics in quasi-perpendicular shocks. However, we currently lack an understanding of key aspects of how these processes operate, with multiple competing theories and sparse data from satellite observations of shocks in space. The experimental platform MagShockZ on the Z Facility aims to create and diagnose these shocks in the laboratory by using the Z Beamlet laser to drive a high-Mach-number collisionless shock through a strongly driven magnetized plasma flow generated by an exploding wire array. The Laser Imaging on Z (LIONZ) diagnostic provides essential insight to the structure and propagation of the shock and its evolution with multi-frame 2D and streaked 1D shadowgraphy images. LIONZ results from the most recent experiment, which show strong evidence of a magnetized collisionless shock, will be discussed.

*This work is supported by the NNSA Center of Excellence under cooperative agreement number DE-NA0004146.
*SNL is managed and operated by NTESS under DOE NNSA contract DE-NA0003525.

Kinetic Investigation of the Effects of Emission Mechanisms on Inverse Sheath Formation*

Bingqing Wang and and Peng Zhang[a]

Department of Nuclear Engineering and Radiological Sciences, University of Michigan, Ann Arbor, Michigan 48109-2104, United States
(bqwang@umich.edu)

Strong electron emission from plasma-facing surfaces can produce an inverse sheath that returns part of the emitted electron population to the wall [1]. This work uses the electrostatic particle-in-cell code EDIPIC [2] to investigate how different emission and collision mechanisms affect inverse-sheath formation and stability. A prescribed-emission model based on Campanell's approach is first used as a benchmark [1]. The model is then extended to include energy-dependent, electron-impact secondary electron emission[3], thermionic emission and photoemission [4,5].

Preliminary results show that suppressing emission from low-energy incident electrons reduces the secondary-electron return flux and eliminates the near-wall potential barrier, causing a transition from an inverse sheath to a classical-like sheath. This demonstrates that sheath behavior depends on the incident-electron energy distribution. Future simulations will compare secondary electron emission with thermionic emission and photoemission. The effects of ion-neutral collisions will also be investigated by comparing the current BGK treatment with an explicit charge-exchange collision model. The study aims to identify how emission physics and ion charge-exchange collisions control inverse-sheath formation, stability, and fluctuations.

*Work supported by the Air Force Office of Scientific Research (AFOSR) Grant Nos. FA 9550-22-1-0523 and FA9550-26-1-B352, and National Science Foundation (NSF) Grant No. 2516752.

References

[1] M. D. Campanell and M. V. Umansky, Phys. Rev. Lett. 116, 085003 (2016)
[2] D. Sydorenko, Ph.D. thesis, University of Saskatchewan (2006)
[3] J. R. M. Vaughan, IEEE Trans. Electron Devices **36**, 1963 (1989).
[4] Y. Zhou and P. Zhang, J. Appl. Phys. 130, 064902 (2021).
[5] Y. Zhou, and P. Zhang, J. Appl. Phys. 127, 164903 (2020).

Circuit-Induced Transients and Ion Energy Control in Pulsed-Bias Capacitively Coupled Plasmas*

Yeon Geun Yook, and Mark J. Kushner

Department of Electrical Engineering and Computer Science, University of Michigan, Ann Arbor, Michigan, USA (ygyook@umich.edu, mjkush@umich.edu)

Pulsed-bias capacitively coupled plasmas (CCPs) are widely used in advanced semiconductor etching to control ion energy delivery and feature-profile. However, intervening circuit components can distort the programmed radio-frequency (RF) voltage before it reaches the powered electrode. Even with an impedance-matching network tuned under quasi-steady conditions, time-varying plasma impedance, stored circuit energy, and blocking-capacitor charging can cause transient distortions during pulse transitions [1,2].

In this work, the consequences of circuit-induced transients on ion energy delivery and cryogenic SiO_2 etching were computationally investigated in pulsed-bias dual-frequency CCPs sustained in Ar/HF mixtures. A 5 MHz bias was applied through a π-type matchbox tuned under quasi-steady conditions and pulsed at 50% duty cycle. The effects of rise/fall times, blocking capacitance, and pulse period on RF power delivery, stored energy, DC self-bias, and ion energy and angular distributions (IEADs) were evaluated.

Circuit transients delayed quasi-steady power delivery during the ON-phase and sustained a residual electrode response after bias turn-off. Compared with late-ON distributions, ON-phase-averaged IEADs exhibited an extended low-energy tail and broader angular spread. During the early OFF-phase, residual energetic ions continued to reach the wafer, enabling ion-assisted etching even after bias turn-off. Feature-scale simulations demonstrated changes in cryogenic etch rates and profiles. These results highlight the importance of circuit dynamics and transient power delivery in translating programmed RF bias conditions into wafer-level ion energy control.

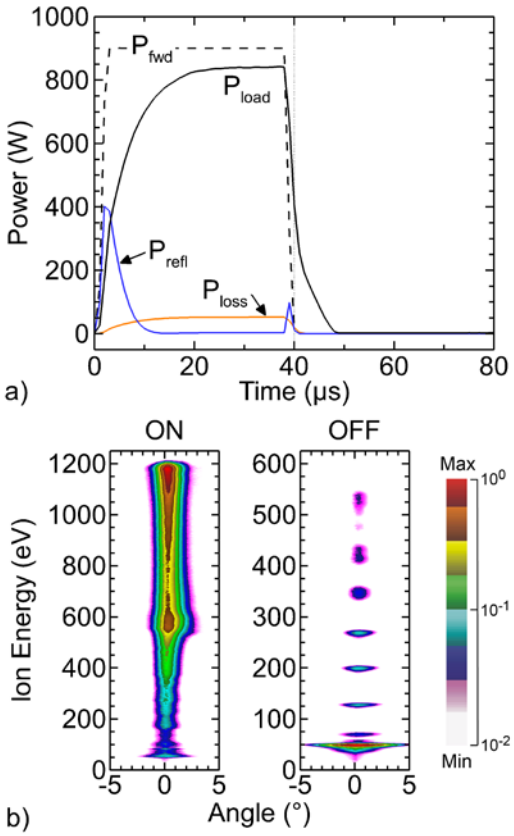


Figure 1 - Circuit-induced transients in RF power and ion energy delivery. (a) Time-dependent forward (P_{fwd}), load (P_{load}), reflected (P_{refl}), and circuit-loss (P_{loss}) powers during a pulse cycle. (b) ON- and OFF-phase-averaged ion energy and angular distributions (IEADs) onto the wafer.

*Work supported by Samsung Electronics.

References

[1] F. Schmidt, T. Mussenbrock and J. Trieschmann, Plasma Sources Sci. Technol. **27**, 105017 (2018).
[2] S. Yu, Z. Chen, Y. Wang, Z. Chen, Z. Wang, W. Jiang, Y. Zhang and J. Schulze, Plasma Sources Sci. Technol. **35**, 025006 (2026).

Experimental Characterization of a Co-Axial Electrodeless Magnetoplasmadynamic Thruster*

Grace Zoppi and Benjamin Jorns
Department of Aerospace Engineering at the University of Michigan (gzoppi@umich.edu)

One of the key metrics for advanced electric propulsion concepts is high power densities enabling high power levels without employing prohibitively large thruster technologies. The Applied Field MPD (AF-MPD) thruster, a type of Lorentz force accelerator, has long been considered a leading choice for this purpose. However, one of the largest obstacles to AF-MPD thrusters has been thruster lifetime. The DC electrodes on these devices are subject to an extreme plasma environment and thus erode rapidly. To mitigate this issue, the Plasmadynamics and Electric Propulsion Laboratory has previously conducted research into utilizing a Rotating Magnetic Field (RMF) to inductively drive the azimuthal current, a major component of the Lorentz force generation in a nominal AF-MPD thruster. This has created a new thruster architecture which we have coined the electrodeless magnetoplasmadynamic (E-MPD) thruster.

In a previous test campaign, we demonstrated the performance of a three-phase RMF-driven thruster in a continuous-wave operation and measured a peak efficiency of 2.6% and specific impulse of 575s on xenon [1]. Given this limited performance, a steady state CFD model was developed to illuminate design strategies to improve thruster performance. These design strategies motivated an annular E-MPD design, a pivot from the previously tested conical geometries [2]. The new design repurposes the magnetic circuit of a Hall-effect thruster to produce applied magnetic fields while embedding RMF antennas in the inner and outer channel walls to enhance the RMF strength. The annular geometry also removes low-current centerline regions and increases the mean thruster radius without increasing thruster size. The first experimental characterization of the 4.5kW annular E-MPD thruster is presented though the application of a suite of diagnostics, including a retarding potential analyzers, Langmuir probes, and current transducers to measure the ion velocity distribution, plasma potential, and RMF waveforms, respectively. These results are compared with those from the conical prototype to assess improvements and develop RMF-driven thrusters.

*Work supported by NASA Grant 80NSSC24K1334

References

[1] C Sercel, “Characterization of Performance and Current Drive Mechanism for the Rotating Magnetic Field Thruster,” PhD thesis. University of Michigan. (2023).
[2] G Zoppi, T Gill, C Sercel, and B Jorns, “The Design and Characterization of a Co-Axial Electrodeless Magnetoplasmadynamic Thruster,” AIAA SCITECH 2025 Forum. (2024). https://doi.org/10.2514/6.2025-2039.

PFOA Degradation in Water: Long-Time-Scale Modeling Investigation*

Jisu Jeon[a], Tiago C. Dias[b], Xuefei Qiu[c], Stephen Olson[d],
Selma Mededovic Thagard[c] and Mark J. Kushner[e]

(a) Department of Nuclear Engineering and Radiological Sciences, University of Michigan, Ann Arbor, Michigan 48109-2122, USA (jisujeon@umich.edu)
(b) Department of Applied Physics, Eindhoven University of Technology, Eindhoven, The Netherlands (t.cunha.dias@tue.nl)
(c) Department of Chemical and Biomolecular Engineering, Clarkson University, Potsdam, New York 13699, USA (qiu@clarkson.edu, smededov@clarkson.edu)
(d) 3M Company, Saint Paul, Minnesota, 55144, USA (saolson@mmm.com)
(e) Department of Electrical Engineering and Computer Science, University of Michigan, Ann Arbor, Michigan 48109-2122, USA (mjkush@umich.edu)

Per- and Polyfluoroalkyl Substances (PFAS), a sub-group of fluorinated organic compounds, are characterized by strong carbon-fluorine (C-F) bonds that render them highly persistent in the environment [1]. Atmospheric pressure plasmas (APPs) have shown effective treatment of certain PFAS at the gas-liquid interface by the incident flux of electrons, ions, radicals and photons as well as in the in-liquid bulk solution by solvated electrons. A validated PFAS degradation mechanisms would aid in optimizing PFAS degradation from water.

In this work, a mechanism for PFOA degradation in water initiated by fluxes from an APP has been developed and implemented in a 0-dimensional (0-D) model *GlobalKin*. Plasma generated fluxes onto the water were obtained from a 2-dimensional (2-D) model *nonPDPSIM*. The initial 10 ppm of PFOA is degraded by 1 kHz, 200 ns discharge pulses. The fluxes produced by the 2-D model are for APP conditions of -30kV, 1.0 cm of water thickness and 100 μS/cm of water conductivity. A parametric investigation varied voltage and pulse repetition frequency, and water conductivity and thickness. The predicted PFOA degradation are shown in Fig. 1a for a 30 s plasma exposure. When normalized by energy deposition onto the water surface, there is reasonably favorable agreement with experiments, shown in Fig. 1b.

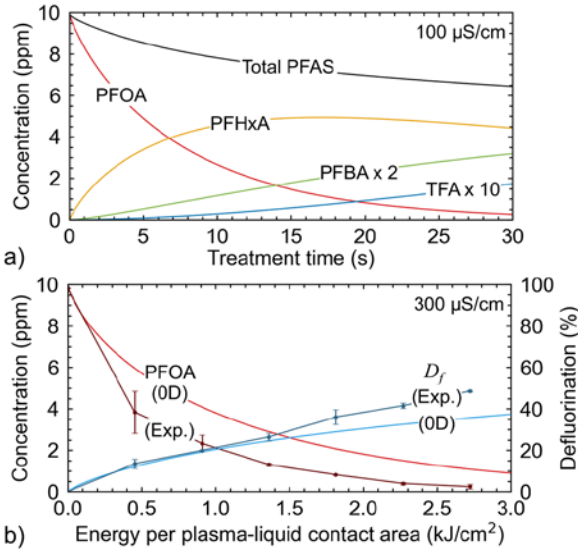


Figure 1 - Concentration of PFOA in water and DHEH fragments (PFHxA, PFBA, and TFA) during plasma exposure. a) *GlobalKin* results for 30 s and b) model and experiments as a function of energy deposition.

*This work was supported by the US Dept. of Energy (DE-SC0020232), Army Research Office MURI (W911NF-20-1-0105), National Science (CBET 2032604) and the 3M Company.

References

[1] S. E. Fenton, A. Ducatman, A. Boobis, J. C. DeWitt, C. Lau, C. Ng, J. S. Smith and S. M. Roberts, Environ. Toxicol. Chem. 40, 606 (2021).

An Investigation of Extreme Low-Density and Low-Speed Solar Wind

Catherine Ballard, Liang Zhao, Jim Raines, Ryan Dewey and Enrico Landi

Department of Climate and Space Sciences and Engineering, University of Michigan (bllrdk@umich.edu)

The coronal origin(s) of slow solar wind, wind that has speeds less than 500 km/s, have not been definitively identified. Most slow solar wind near 1 AU has been found to have average densities between 5 and 10 cm-3, relatively high density ratios of C6+/C5+ and O7+/O6+, and enhanced abundance ratios of elements with low first ionization potential (FIP). However, not all slow solar wind has properties within these ranges. Solar wind disappearance events (Balasubramanian+ 2003), where the solar wind has both extremely low speeds (less than 300 km/s), and extremely low proton densities (less than 1 cm-3), have not yet been fully studied or compared with similar events. We compare the extremely low-density and extremely low-speed solar wind with the more typical slow solar wind using ACE observations from 1998 to 2021. 41 extreme events were identified with a tendency towards occurring during maximums of the solar cycle. Charge state compositions were analyzed for the 27 events that occurred before 2010, showing expected high values for the carbon and oxygen density ratios. However, all 27 events had FIP effect signatures more similar to those of fast solar wind. These charge states are frozen-in close to the solar surface due to rapidly decreasing density at farther distances from the Sun allowing us to infer information about the conditions of the solar atmosphere from data measured at L1. Our results suggest that disappearance events originate somewhere different than typical slow solar wind, with potential origins discussed in this study.

References

[1] C. W. Smith, et al., JGR: Space Physics. **106**, A9. (2001).
[2] P. Janardhan, JAA. **27**, 2 (2006).
[3] V. Balasubramanian, et al., JGR: Space Physics, **108**, A3 (2003).
[4]G. Le et al., GRL, **27**, 14 (2000).
[5]P. Janardhan, et al., JGR: Space Physics, **110**, A8, (2005).
[6] P. Janardhan, et al., A&A, **488**, 1 (2008).
[7] R. von Steiger and T. H. Zurbuchen, JGR, **116**, A01105, (2011).

Micropinch Characterization on Hybrid X-pinches using the PERSEUS xMHD Code*

Shane Keiser and Ryan McBride

University of Michigan, Department of Nuclear Engineering and Radiological Sciences
(sakeiser@umich.edu, mcbrider@umich.edu)

Hybrid X-pinches have previously been studied as point-like radiation sources, due to their spatial extent being an order of magnitude smaller than typical Z-pinches. In recent experiments, beyond soft- and hard- X-ray emission, hybrid X-pinches on low-mass polyethylene fiber loads have led to the observation of radial proton acceleration, of which the emission mechanism is not well understood [1,2]. The proton fluence was high enough to elicit use of the platform for proton radiography, which was successfully demonstrated in Ref. [1].

These observations have given yet more motivation to find ways to model plasmas with a combined fluid-kinetic description, with one such attempt being the RIOT code under development at Los Alamos National Laboratory.

We ran simulations in the PERSEUS xMHD code [3] to probe the evolution of plasma at a micropinch with similar parameters as in Refs. [1,2]. Work was also done to determine the Knudsen number and plasma coupling parameter, to test heuristic validity that will aid the plasma transport side of the RIOT code's development.

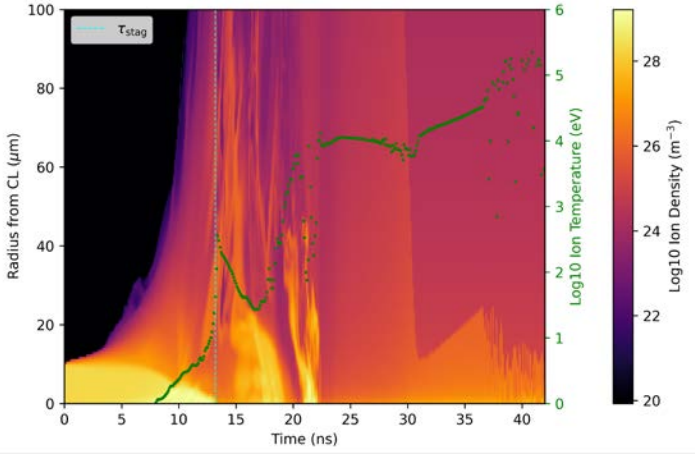


Figure 1 – Density heatmap showing averaged density across a 3 micron slice of a prominent micropinch from a 2D PERSEUS simulation. The simulation parameters match those used in Refs. [1,2] as best as possible. The green scatter shows ion temperatura through the simulation, and the peak at stagnation time (13 ns) agrees roughly with the emission of soft X-rays in experiment.

*Work supported by the LANL LDRD program under project 20260060DR, and by the DOE-NNSA under Cooperative Agreement DE-NA0004148. LANL is operated by Triad National Security, LLC, for the DOE-NNSA under Contract 89233218CNA000001.

References

[1] D. Klir et al., Phys. Rev. Lett. 136, 145101 (2026).
[2] D. Klir et al., Phys. Plasmas 33, 072701 (2026).
[3] C. E. Seyler and M. R. Martin, Phys. Plasmas 18, 012703 (2011).

On the Evolution of the Magneto-Rayleigh Taylor Instability in Cylindrical Geometry*

Corey Gui, Ryan D. McBride, Nicholas M. Jordan and Peng Zhang

University of Michigan (coreygui@umich.edu)

Z-pinch and implosions provide powerful platforms for reaching high-energy-density regimes. These implosions are used for plasma diagnostics and high-energy-density science and form the underlying compression mechanism in magnetized liner inertial fusion (MagLIF). Their performance, however, is fundamentally limited by the magneto-Rayleigh–Taylor instability (MRTI), which degrades stagnation pressure and disrupts implosion symmetry. Techniques such as dynamic screw pinches [1], Helmholtz coils, and gas-on-liner configurations [2] have been proposed to mitigate MRTI by modifying the background magnetic field during the implosion, with experiments demonstrating reduced instability growth. Existing cylindrical MRTI theories, however, generally focus on linear stability [3] or prescribe specific background magnetic-field configurations, limiting their ability to describe the influence of more general field profiles.

In this work, we extend the variational theory of Ruiz [4] to cylindrical geometry, developing a model of MRTI on a cylindrical fluid column. The model retains arbitrary helical modes and a radially varying axial–azimuthal background magnetic field, allowing the effects of magnetic-field geometry on linear growth and nonlinear mode coupling to be studied.

* Work supported by NSF Grant No. PHY-2205608 and DOE-NNSA Cooperative Agreement DE-NA0004148.

References

[1] P. C. Campbell et al., Physics of Plasmas **28**, 082707 (2021).
[2] J. M. Chen, Ph.D. dissertation, University of Michigan (2025).
[3] M. R. Weiss et al., Phys, Plasmas, **21**, 122708 (2014).
[4] D. E. Ruiz, Phys. Plasmas, **27**, 022121 (2020)

Abstracts: Poster Session II

Effect of Orbital Angular Momentum on Wake Instabilities in a Laser Wakefield Accelerated Beam*

Victoria Collemi[a], Qian Qian[b], Neil Beri[b], Milos Burger[b], Leah Hartman[b], Karl Krushelnick[b] and Alexander G. R. Thomas[b]

(a) Department of Nuclear Engineering & Radiological Sciences (vcollemi@umich.edu)
(b) Gerard Mourou Center for Ultrafast Optical Sciences (qqbruce@umich.edu, nebe@umich.edu, milosb@umich.edu, lghart@umich.edu, kmkr@umich.edu, agrt@umich.edu)

Advancements in orbital angular momentum (OAM) have enabled greater tunability to the spatiotemporal structure of laser pulses. This is typically accomplished through specific combinations of Laguerre-Gaussian (LG) modes, which contain a helical phase front. Recently, Longman et. al. experimentally demonstrated that a superposition of LG modes (i.e. spatiotemporal light springs) can achieve relativistic laser intensities and produce helical plasma waves.[1] In the context of Laser Wakefield Acceleration, OAM allows for more complex wake structures and trapped particle confinement schemes. The rotational dynamics of the wake in OAM LWFA may enable positron acceleration, which is difficult to achieve in traditional (Gaussian) LWFA. However, OAM also introduces a rotational component to common LWFA instabilities.[2]

In Gaussian LWFA, phenomena including current filamentation instability (CFI), self-modulation instability (SMI), and laser hosing can be analyzed through the lens of cylindrical symmetry. The presence of OAM breaks this symmetry, requiring a more general 3D azimuthal symmetry to fully describe such instabilities. This introduces an added degree of freedom to how these instabilities can evolve during the acceleration. Understanding how OAM affects the development of these rotationally modified phenomena is significant to developing future plasma colliders.[3]

Current studies of LWFA studies (Gaussian or OAM) typically focus either in the linear or nonlinear (e.g. blowout) regime. However, there is a gap in the literature regarding the critical transition region and the onset of these OAM-induced instabilities. To investigate the effect of OAM on LWFA wake instabilities and the transition region, fully relativistic electromagnetic particle-in-cell code OSIRIS will be utilized to simulate a single pulse OAM LWFA propagating through an underdense background plasma profile. The data generated will be processed using a conformal mapping technique to reveal the evolution of the wake structures as the pulse progresses from the linear to the blowout regime (i.e. increasing normalized laser intensity).[4][5]

*Work supported by the NSF and AFOSR.

References

[1] A. Longman, D. Attiyah, E. S. Grace, C. Gardner, T. Suratwala, G. Tham, C. Harthcock, R. Fedosejevs, and F. Dollar, Nat. Photon. **20, 843** (2026).
[2] J. Vieira and J. T. Mendonça, Phys. Rev. Lett. **112, 215001** (2014).
[3] Q. Qian, M. Li, Y. Ma, P. T. Campbell, C-H. Chang, E. Denis, N. Ernst, R. Fedosejevs, B. Hou, A. James, M. W. von der Leyen, K. Krushelnick, C. Kuranz, A. Longman, A. Maksimchuk, J. Nees, P. Norreys, T. Nutting, J. B. Ohland, J. P. Palastro, A. G. R. Thomas, R. Timmis, L. Willingale, and M. Burger, **arXiv:2608.15039** (2026).
[4] D. G. Pires and N. M. Litchinitser, Engineering **17, 31** (2022).
[5] D. Yang, X. Hu, J. Dou, Z. Yang, Z. Zhao, and Z. Liu, J. Opt. **24, 055701** (2022).

Investigation of Oxygen Resilience of Thermionic Emitters for Electric Propulsion*

Carter Krumins and Benjamin Jorns

University of Michigan Department of Aerospace Engineering (ckrumins@umich.edu)

Many Electric Propulsion (EP) systems rely on noble gases carried onboard, whereas propellants collected through In-Situ Resource Utilization (ISRU) from planetary atmospheres or extraterrestrial ice water could reduce the expensive launch masses from Earth. Usage of these resources however comes with the caveat of requiring compatibility with oxygen. This compatibility has been shown as particularly difficult in the conventional hollow cathode architectures that supply electrons for thruster operation. Gallagher's 1969 study of lanthanum hexaboride (LaB_6) cathodes showed that oxygen harshly suppresses thermionic emission, and that resistance to poisoning increases with cathode temperature [1]. Higher operating temperatures, however, commonly accelerate material loss to an extreme. In light of these challenges, a need arises for development of emitters that sustain electron emission while resisting degradation in oxygenated environments.

This works presents the design of a new cathode test setup to evaluate promising candidates for thermionic emitters that are robust to an oxygen-rich environment. The design incorporates an interchangeable puck mount, a graphite heater for radiative heating, and a spring-loaded mount to accommodate expansion. The experimental setup is outlined including initial current-voltage measurements, pyrometry, and Langmuir probe diagnostics to relate cathode performance to emitter temperature and plasma conditions. Initial results from characterization with hafnium oxide are presented.

*Work supported by DARPA through the CASTOR program.

References

[1] Gallagher, H. E., "Poisoning of LaB_6 Cathodes," Journal of Applied Physics, 40(1), 44–51 (1969). doi:10.1063/1.1657092.

Dynamics of Charge Conduction in Water Layers Formed During Cryogenic Etching of HAR SiO_2 Features*

Chenyao Huang[a], Yeon Geun Yook[a], Yifan Gui[a], Steven C. Shannon[b] and Mark J. Kushner[a]

(a) University of Michigan, Ann Arbor, MI
(b) North Carolina State University, Raleigh, NC
(chenyaoh@umich.edu, ygyook@umich.edu, evangyf@umich.edu, scshanno@ncsu.edu, mjkush@umich.edu)

During the fluorocarbon plasma etching of dielectric materials, differential charging within features arises from the disparity between the arrival onto the wafer of energetic ions with narrow angular spread and low-energy electrons with broad angular distributions. The resulting intra-feature electric fields can deflect particle trajectories, leading to defect formation and reduced etch rates. Cryogenic plasma etching (CPE) is being investigated as an alternative due to its high etch rate and attractive sidewall profile control for high aspect ratio (HAR) features. During cryogenic etching of dielectrics using HF containing gas mixtures, water layers containing solvated HF form along the feature sidewalls in addition to charge deposition from incident charged particle fluxes. These liquid layers may have significant conductivity due to the ionic solute concentrations (e.g., H_3O^+ and F- when solvating HF in water). This conductivity can alter the potential distributions within the feature by conducting externally deposited charges and facilitating self-polarization.

In this work, we computationally investigated charging dynamics including conductive layers for pre-formed SiO_2 features, and during plasma etching of HAR SiO_2 features using Ar/HF gas mixtures in multi-frequency capacitively coupled plasmas. Feature evolution is modeled and using the 3D voxel-based Monte Carlo Feature Profile Model (MCFPM). Fluxes and energy angular distributions (EADs) of incident species are produced by the reactor-scale Hybrid Plasma Equipment Model (HPEM). The MCFPM samples incident fluxes to statistically launch pseudoparticles representing charged and neutral species, which are tracked until they interact with solid materials. We have developed and integrated modules into the MCFPM to account for charge conduction and redistribution within conductive water layers during etching. Our results indicate that these highly conductive, thin layers transform local maxima of electric potential into a broadened profile with lower peak potentials within the features. During SiO_2 etching, the water layer counteracts externally deposited charges through the redistribution of external and intrinsic charges, resulting in a reduced electric potential that correlates inversely with the intrinsic charge densities represented by the dissolved ions.

*This work was supported by the Department of Energy Office of Fusion Energy Sciences (DE-SC0024545) and Samsung Electronics.

Chemical Vapor Deposition of Delta-Doped Diamond with a NIRIM Type Reactor

Alex Loomis[a], Logan Crooks[a], Andrew R. Kirkpatrick[a], Jonas N. Becker[a], Shannon S. Nicley[a,b]

(a) Quantum Optical Devices Laboratory (QuOD), Michigan State University (loomisa6@msu.edu)
(b) Fraunhofer USA Inc, Center Midwest, Coatings and Diamond Technologies Division
1449 Engineering Research Ct. East Lansing, MI 48824, USA

In recent decades, improved technology and information theory have brought us closer to a second quantum revolution that utilizes quantum mechanics to its full potential [1]. Diamond is a great platform for optically active defects for quantum information processing (QIP) applications, able to host hundreds of different color centers within its wide bandgap. It is transparent from infrared to ultraviolet wavelengths and growth with ^{12}C-enriched methane allows for nuclear spin-free material, suppressing spin-spin interactions to improve coherence times. Isolating individual color centers with a favorable local environment is made easier by growing very thin layers of doped diamond called delta-doped layers.

Diamond growth through chemical vapor deposition (CVD) enables the fabrication of high quality diamond with precise control over precursor gases. Doping with silicon creates SiV color centers, a well-studied defect in diamond. Photoluminescence spectra of the SiV ensembles can be used to quickly assess the quality of the grown film. Growth of this material has been achieved through a NIRIM-type diamond reactor, (figured top right). Diamond growths have been conducted (figured bottom right) under varying conditions to find favorable parameters for single crystal diamond growth. The reactor is based on a space constrained design [4] and modified for higher vacuum to ensure an extremely low leak rate to achieve very high sample purity. Varying Si/C ratios have been studied to define an upper limit on silicon incorporation before growth quality suffers. Conditions for high-quality diamond growth have been determined and reproduced reliably. Currently, effects of surface preparation and low methane concentration on the film's roughness are being studied. In this poster, I will introduce the parameters that affect delta-doped layer growth and the potential of in-situ silicon doping during CVD.

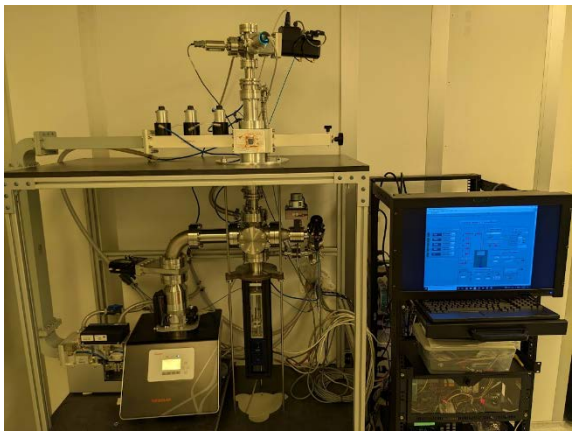


Figure 2 - Diamond System 11 (DS11).



Figure 1 - Chemical vapor deposition of diamond in DS11.

References

[1] J.P. Dowling and G.J. Milburn, *Philos. Trans. R. Soc. A* **361,** 1655 (2003)**, [2]** J. N. Becker, Ph.D. Thesis, Saarland University (2017), **[3]** C. Weinzetl, *et al., Phys. Rev. Lett.* **122**, 063601 (2019), **[4]** E.H. Thomas *et al., AIP Adv.* **8**, 035325 (2018).

Current Crowding and Contact Resistance in Anisotropic 2D Devices*

Md Arifuzzaman Faisal, Peng Zhang

Department of Nuclear Engineering and Radiological Sciences, University of Michigan, Ann Arbor, Michigan, 48109-2104, USA (faisalmd@umich.edu)

Atomically thin 2D semiconductors have excellent electrostatic capability and strong gate control of the channel which enables transistor scaling [1]. However, charge injection into the channel from metal contacts is inherently anisotropic for most 2D semiconductors as they conduct much better in the plane than out of the plane [2]. Consequently, for a top-contacted transistor, current is concentrated near the surface of the channel, causing significant current crowding to create hot spots. Thus, contact resistance is not only governed by the interface properties, but also by the combined effects of the conductivity tensor and contact dimensions. Most existing models for thin film contacts have assumed isotropic transport or utilized a transmission line method (TLM) approximation, which is not capable of accurately representing this combined effect of field redistribution on contact resistance [3]. For DC transport, we develop an exact two-dimensional field solution by considering both an anisotropic electrode and semiconductor channel, a resistive interface, and finite boundaries. Our exact field model shows that anisotropic conductivity, interface resistance, and geometry affect the current flow and current crowding, and therefore modify contact resistance. The exact solution shows how the transfer length, and contact resistance differ significantly from TLM predictions. Exact field solutions show the limits within which TLM can be used successfully and when it fails to describe the current transfer behavior. Finally, we compare our predictions with published contact resistance measurements and find good agreement [4,5]. We also analyze AC contact resistance in anisotropic materials by extending our anisotropic DC contact framework [2] to AC conditions using the formulation of Ref. [6] and solving the anisotropic Helmholtz equation. The AC solution shows how anisotropy modifies current redistribution, current crowding, and contact impedance over frequency.

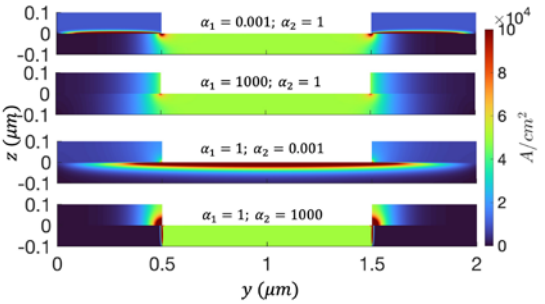


Figure 1 - Current density distribution for different anisotropy ratios, with fixed $I_{total} = 50\ \mu A/\mu m$, $\rho_{1z} = \rho_{2z} = 1 \times 10^{-5} \Omega.m$,

*The work is supported by the Air Force Office of Scientific Research (AFOSR) Award Nos. FA9550-22-1-0523 and FA9550-26-1-B352.

References

[1] X. Hou et al., ACS Nano, vol. 19, pp. 20589-20598, (2025).
[2] M. A. Faisal and P. Zhang, ACS Appl. Electron. Mater., vol. 8, pp. 854-864, (2026).
[3] P. Zhang, Y. Y. Lau, and R. M. Gilgenbach, J. Phys. D: Appl. Phys., vol. 48, p. 475501, (2015).
[4] C. D. English, G. Shine, V. E. Dorgan, K. C. Saraswat, and E. Pop, Nano Lett., vol. 16, pp. 3824-3830, (2016).
[5] S. Song et al., Nat. Commun., vol. 13, Art. no. 4916, (2022).
[6] F. Antoulinakis and Y. Y. Lau, J. Appl. Phys., vol. 127, Art. no. 125107, (2020).

Simulation and Experimental Demonstration of an Overmoded X-band Magnetically Insulated Line Oscillator*

Adam Brusstar and Nicholas M. Jordan

Department of Nuclear Engineering and Radiological Sciences, University of Michigan, Ann Arbor
(anbruss@umich.edu)

The magnetically insulated line oscillator (MILO) [1] is a high power microwave source which confines electrons using the self-generated magnetic field of the current drawn by the device, rather than an external magnet. To address pulse shortening and power handling concerns with conventional MILO configurations at high frequency, an overmoded X-band MILO (OXMILO) was designed to operate using the asymmetric hybrid electromagnetic HEM_{11} and HEM_{21} modes [2]. Particle in cell simulations were performed in CST microwave studio as shown in figure 1, which predict an output power of 18 MW at 9.6 GHz when driven with an input voltage and current of 300 kV and 9 kA.

Preliminary experiments performed on the Michigan Electron Long Beam Accelerator (MELBA) and Repetitive Experimental Platform (REP) Marx banks revealed substantial deficiencies in the mechanical alignment system for the anode and cathode, which negatively impacted power output, mode stability and maximum pulse length. To address concerns raised in the initial set of experiments, a novel precision positioning and alignment system using exact constraint principles was fabricated, along with a shorter insulator stack having an improved electrostatic design [3] that reduced the maximum electric field from 28 kV/cm to 16 kV/cm. Experimental validation of this design is ongoing.

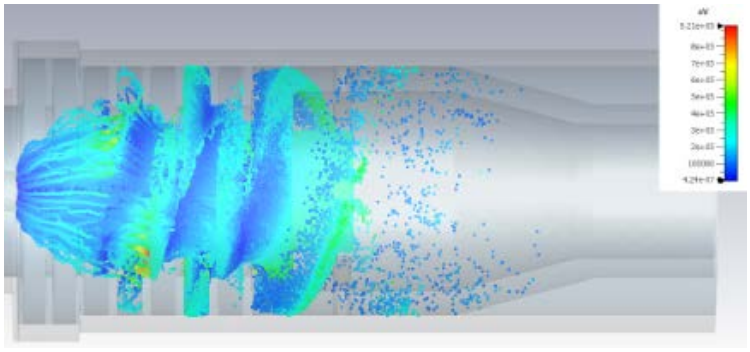


Figure 1 – Simulation showing helical electron spoke formation when operating in an elliptically polarized HEM_{21} mode.

Additional improvements currently being explored include an extractor with optimized feedback from the inner conductor support posts that has been shown in simulation to increase the output power from 18 MW to 46 MW, helical Bragg reflector chokes to control the polarization of the asymmetric modes, and a slow-to-fast wave impedance taper.

*Work supported by the Office of Naval Research grant number N00014-23-1-2143.

References

[1] M. C. Clark, B. Marder and L. Bacon, Appl. Phys. Lett. **52**, 78 (1988).
[2] R. Revolinsky, A. Brusstar and N. M. Jordan, IEEE Trans. Plasma Sci. **53**, 3269 (2025).
[3] W. Stygar, et al., Phys. Rev. ST Accel. Beams. **8**, 0505401 (2005).

HEROICS: A SWaP-Efficient Triple Coincidence Time of Flight Plasma Spectrometer*

Sarah R. Feldman, Tyler J. A. Eddy, Ben Miller, Isaac Fertig, Jay Phull, Jaccob M. Bell, Louis G. Marr, Fernando A. Saca, Jim M. Raines, and Sue T. Lepri

University of Michigan, Climate and Space Sciences and Engineering (sarfeldm@umich.edu)

From studying the composition of solar wind to planetary magnetospheres, in-situ plasma particle measurements are a cornerstone of any space mission. However, such instruments often have to balance the high voltages and physical space needed to achieve the intended resolution against other payloads on a spacecraft. We have developed **HEROICS** (**H**igh-resolution **E**nergy-**R**esolving **O**mni-directional **I**on **C**omposition **S**pectrometer, formerly known as **TFIPS**, **T**riple **F**ast **I**maging **P**lasma **S**pectrometer) in response to be a SWaP (Size, Weight, and Power) efficient solution to measuring heavy ions.

At 5kg in mass, 5W in power consumption, and a little over 6U in size, HEROICS is a triple-coincidence plasma mass spectrometer that takes heritage from the Fast Imaging Plasma Spectrometer (FIPS) [1], which flew on NASA's MESSENGER mission and collected invaluable ion composition observations of the Hermitian magnetosphere from 2011-2015 [2]. HEROICS uses the same electrostatic analyzer design, remade with now-available manufacturing techniques, with a partially redesigned time of flight chamber and an added energy-resolving avalanche photodiode (APD) detector floated in a miniature high-voltage bubble. Ion optical design and performance analysis has been done, while prototyping and calibration efforts are ongoing.

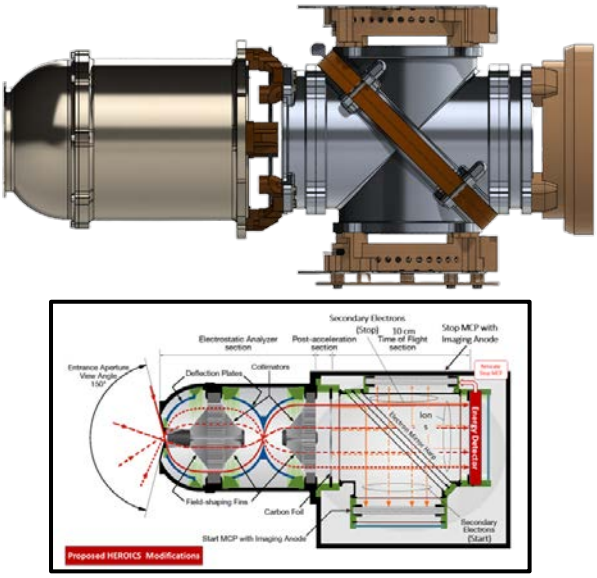


Figure 1 - CAD Model of HEROICS with proposed changes from FIPS highlighted

These improvements will allow HEROICS to measure the kinetic properties of ions from 1-60 amu/e, such as H^+, He^{1-2+}, C^{1-6+}, O^{4-8+}, Na^+, Si^+, S^+, Ca^+, Fe^{8-16+} and ions of H_2O, CO_2, NH_3, and CH_4, from energies of 50 eV/e to 20 keV/e. This range makes it well suited to answer critical science questions about different plasmas sources in planetary magnetospheres, wave-particle interactions, and global convection patterns, as well as a wide range of phenomena in the solar wind.

*This material is based upon work supported by the National Science Foundation Graduate Research Fellowship Program under Grant No. DGE 2241144.

References

[1] Andrews, G. B. et al., Space Science Reviews. **131**, 523–556 (2007).
[2] Raines, J. M. et al., JGR: Space Physics. **118**, 1604–1619. (2013).

Modeling the Longitudinal Dependence of Radiation Belt Electron Dynamics at Earth and Jupiter

Josh Fung[a], Zhi-gu Li[a], Weichao Tu[a], Qianli Ma[b], Jinbei Huang[a]

(a) Climate and Space Sciences and Engineering, University of Michigan
(b) Department of Atmospheric and Oceanic Sciences, UCLA

Planetary radiation belts exhibit longitudinal asymmetries governed by their magnetic topologies and physical obstacles such as moons. At Earth, magnetic anomalies near the surface, such as the South Atlantic Anomaly, introduce significant longitudinal dependence in the bounce loss cone. This drives the "windshield wiper" effect, where quasi-trapped azimuthally drifting electrons are preferentially precipitated into the upper atmosphere at certain longitudes where the bounce loss cone becomes large [1]. Jupiter features similar local magnetic anomalies near its surface, also suggesting a longitude-dependent precipitation mechanism [2]. However, the Jovian radiation environment is further complicated by the presence of moons. The orbital planes of the Jovian moons are highly inclined with respect to Jupiter's magnetic equator, and consequently these moons traverse through a range of M-shells. This orbital geometry creates highly localized, instantaneous electron dropouts, known as "moon sweeping", that are dependent on both the specific magnetic longitude and M-shell the moon currently occupies [3].

To comprehensively model these effects, we employ a 3-dimensional Fokker-Planck solver operating in equatorial pitch angle, magnetic longitude, and radial M-shells. Statistical whistler-mode wave models are used to derive realistic pitch-angle diffusion coefficients [4]. By combining azimuthal drift, pitch-angle diffusion, radial diffusion, and longitudinally dependent moon sweeping, we map the spatial distributions of electron flux dropout in the Jovian magnetosphere. These simulation results provide a comparative framework for understanding how magnetic topologies and moons govern radiation belt electron dynamics across different planetary environments.

References

[1] Z.-G. Li, W. Tu, R. Selesnick, and J. Huang, J. Geophys. Res. Space Phys. 129, e2023JA032171 (2024).
[2] D. Grodent et al., J. Geophys. Res. 113, A09201 (2008).
[3] M. Long et al., J. Geophys. Res. Planets 127, e2021JE007050 (2022).
[4] W. Li et al., Geophys. Res. Lett. 53, e2026GL122294 (2026).

Nuclear Fusion Enhancement in Dense Plasmas*

Julian P. Kinney and Scott D. Baalrud

Department of Nuclear Engineering and Radiological Sciences, University of Michigan
(julkin@umich.edu)

Plasma screening due to ions and electrons is well known to enhance nuclear fusion reaction rates. The plasmas in brown and red dwarf stars can exist at modest temperatures $T{\sim}0.05-1\ keV$ and high mass densities of $\rho{\sim}10-10^4\ g/cc$, where theories of nuclear fusion enhancements must account for strong coupling between ions and electron degeneracy (see Fig. 1). Strong ion coupling occurs when the ratio of the potential energy between ions exceeds the average kinetic energy in the plasma and is captured by an ion Coulomb coupling parameter $\Gamma \propto \left(Z^2e^2\rho^{1/3}\right)/k_BT \gtrsim 1$. The degree of electron degeneracy in a plasma is characterized using the ratio of the plasma temperature to the Fermi energy $\Theta = k_BT/E_F$.

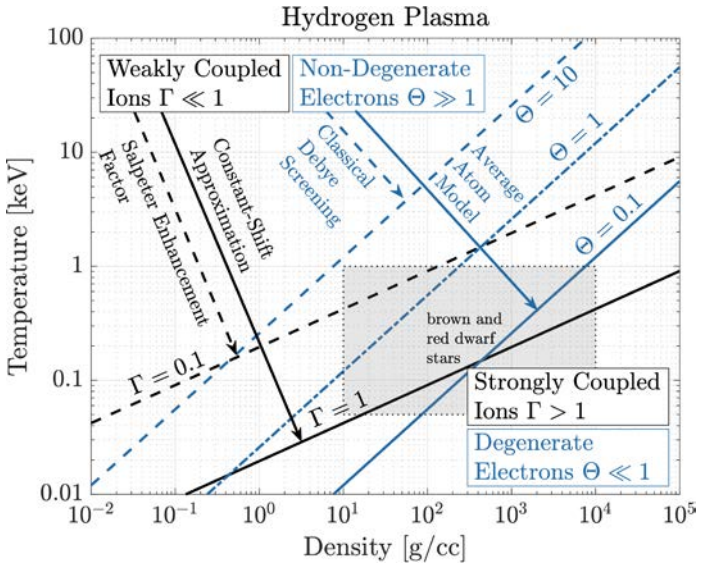


Figure 1 – Descriptions of nuclear fusion enhancements across the plasma density and temperature space can be characterize by considering the ion Coulomb coupling parameter (Γ) and the electron degeneracy parameter (Θ).

Models of enhanced nuclear fusion rates due to plasma screening for weak ion coupling $\Gamma \ll 1$ are typically based on a constant lowering of the Coulomb repulsion between ions at short interparticle distances. This "constant-shift approximation" begins to break down due to strong coupling between the ions. Furthermore, many models of electron screening of nuclear reactions either use non-degenerate, classical plasma description ($\Theta \gg 1$) or assume a fully degenerate state ($\Theta \ll 1$). However, in brown and red dwarf stars, the electrons may exist in the "intermediate screening regime" between these two limits.

This work presents a method for calculating nuclear fusion rates in dense plasmas that includes both strong ion coupling ($\Gamma \gtrsim 1$) and the intermediate screening regime ($0.1 \lesssim \Theta \lesssim 10$). Specifically, the quantum tunneling probability is calculated using the Wentzel-Kramers-Brillouin approximation, but where the interactions between ions takes place through the potential of mean force. In regimes where intermediate electron screening occurs, the model uses the potential of mean force derived from an orbital-based average-atom model that contains a quantum-mechanical description of the electrons.

*This work is funded by DOE NNSA Stockpile Science Graduate Fellowship through cooperative agreement DE-NA0004185.

Two-dimensional Quantum-Mechanical Analysis of Ion-Enhanced Thermionic and Thermo-Field Emission and the Peak-Current Phenomenon*

Wanglim Song and Peng Zhang

Department of Nuclear Engineering and Radiological Sciences, University of Michigan
(wlsong@umich.edu, umpeng@umich.edu)

In this work, we develop a framework for ion-enhanced thermionic and thermo-field emission, building on previous thermionic, quantum field-emission, resonant-tunneling, and multidimensional ion–surface models. [1-6] The framework combines one-dimensional quantum transmission calculations with an axisymmetric quasi-two-dimensional description and radial integration of the current-density distribution. Numerov calculations resolve over-barrier transport and quantum tunneling. [3] Ion-induced enhancement is strongly localized, with thermionic, nonresonant-tunneling, and resonant-tunneling contributions governed by field strength, cathode temperature, and ion–surface separation. Radial integration yields the net additional current associated with a single ion.

Peak emission occurs near the ion position where the two potential-barrier maxima surrounding the ion-induced well become equal. This condition minimizes the larger barrier and yields an empirical relation, $L_c[\mathrm{nm}] = 0.8140/\sqrt{F[\mathrm{V/nm}]}$, establishing an $F^{-1/2}$ scaling for the characteristic peak-emission position. Calculations for several cathode materials follow this common trend (Fig. 1). Deviations increase as thermionic emission decreases and resonant tunneling becomes more dominant, governed primarily by temperature at low fields ($F < 1{\sim}$V/nm) and field strength at high fields ($F > 1{\sim}$V/nm). The single-ion current is extended to a bulk ion population by discrete superposition at instantaneous ion positions. This framework is expected to provide insight into microscale gas breakdown and ion-sheath physics.[5]

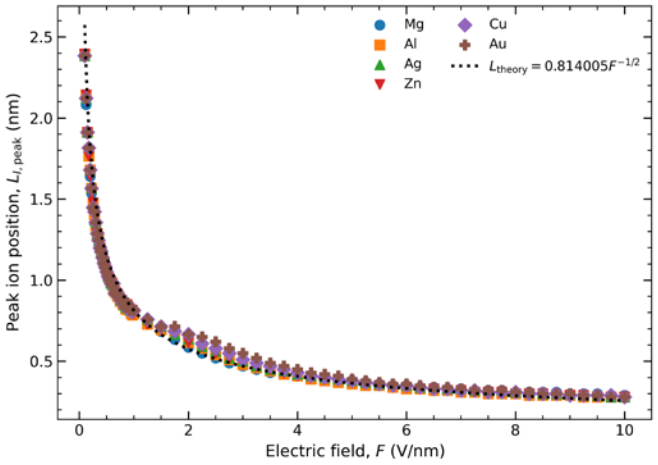


Figure 1 - Peak position L_{peak} as a function of applied electric field F for several cathode materials.

*This work was supported by the Air Force Office of Scientific Research (AFOSR) Grant No. FA9550-26-1-B352, and by National Science Foundation (NSF) Grant No. 2516752.

References

[1] D. B. Go, J. Phys. D: Appl. Phys. 46, 035202 (2013).
[2] Y. Li and D. B. Go, J. Appl. Phys. 116, 103306 (2014).
[3] X. Tan, P. Rumbach, N. Griggs, K. L. Jensen, and D. B. Go, J. Appl. Phys. 120, 213301 (2016).
[4] T. Josso, H. Jouin, C. Harel, and R. Gayet, J. Phys. D: Appl. Phys. 31, 996–1008 (1998).
[5] D. B. Go and A. Venkattraman, J. Phys. D: Appl. Phys. 47, 503001 (2014).
[6] Y. Zhou, R. Ahsan, H. Chae, R. Kapadia, and P. Zhang, Phys. Rev. Applied 20, 014043 (2023).

Simulations and Experiments Measuring Temperature Relaxation Rates in a Strongly Magnetized Antiproton-Electron Plasma*

James C. Welch III[a], Louis Jose[a], Timothy D. Tharp[b], Chris Ø. Rasmussen[c], and Scott D. Baalrud[a]

(a) Nuclear Engineering & Radiological Sciences, University of Michigan, Ann Arbor, Michigan 48109, USA (welchjc@umich.edu)
(b) Physics, Marquette University, Milwaukee, Wisconsin, 53233, USA
(c) Brookhaven Nation Laboratory, Upton, New York 11973, USA

Antimatter experiments sympathetically cool antiprotons using electrons in a Penning-Malmberg trap. In this trap, non-neutral plasmas are confined axially by an applied electric field and radially by a strong applied magnetic field. The Brillouin limit requires that the plasma is strongly magnetized (the gyrofrequency exceeds the plasma frequency) for confinement. Standard kinetic theory fails in the strongly magnetized regime, but a recent kinetic theory [1] appropriate for this regime can predict temperature relaxation rates. Previous experiments have measured temperature anisotropy relaxation rates in pure ion [2] and pure electron plasmas [3]. Applying an oscillating voltage to the confining electrode axially compresses and rarefies the plasma. Driving the plasma at a frequency near certain relaxation rates irreversibly heats the plasma, while off-resonant driving produces a reversible process. By performing this experiment for many applied frequencies, it is expected that the frequencies associated with maximal heating are proportional to certain temperature relaxation rates. These measurements have been made in both physical experiments and molecular dynamics simulations.

* NSF grant award No. PHY-2205506

References

[1] L. Jose et al., Phys. Rev. E (2025)
[2] B. R. Beck, et al., Phys. Plasmas (1996)
[3] F. Anderegg, et al., Phys. Plasmas (2017)

Effects of Back Wall Material in an ECR Magnetic Nozzle Thruster

Ari Eckhaus and Benjamin Jorns

University of Michigan (aeckhaus@umich.edu)

Magnetic nozzle thrusters have long been coveted for their ability to eliminate the neutralizer cathodes commonly found on mature electric propulsion (EP) devices. Removal of the cathode, and its associated power and flow systems, not only simplifies the propulsion system but also, in principle, enables the device to run on a variety of propellants [1]. One particularly promising thruster concept pairs the magnetic nozzle architecture with an electron cyclotron resonance (ECR) plasma heating scheme. By tuning the frequency of an injected RF wave to match the electron cyclotron frequency, ECR can achieve power coupling efficiencies above 90%. Largely because of this effective coupling, ECR magnetic nozzle thrusters can operate in low power regimes (< 50 W). This low power capability, combined with the simplicity provided by the magnetic nozzle, makes ECR magnetic nozzle thrusters promising candidates for small satellite propulsion.

Previous characterizations of ECR magnetic nozzle thrusters have highlighted the importance of materials in contact with the plasma [2]. However, there has been limited investigation into the interaction between the plasma and the back wall of the plasma source region. Indeed, it is expected that the interaction with the back wall is critically important to not only the ECR thruster, but all magnetic nozzle thrusters. As shown in Fig. 1, this is because the magnetic field lines of the nozzle stream directly into the back wall of the plasma chamber. Furthermore, the ECR interaction zone is located a few millimeters from the rear surface, meaning that the heated electrons impinge on the back wall, acting as a power loss mechanism. Additionally, the back wall also serves to direct the injected microwaves into the source region. As a result, changes to back wall material may also cause changes in the microwave power delivered to the plasma. In fact, manufacturing back wall entirely from a conductive material will short the microwave delivery circuit, preventing the thruster from operating.

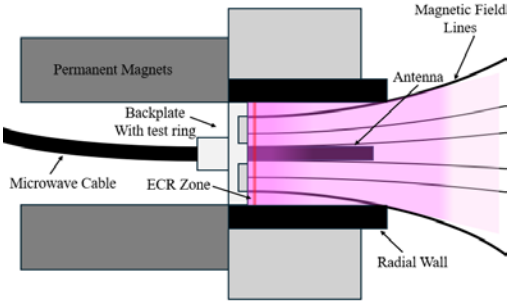


Figure 1 – Notional cross section of a typical ECR magnetic nozzle thruster.

We therefore adopt the approach, shown in Fig. 1, of adding rings of different materials to the surface of a base boron nitride backplate. In this way, we decouple changes in microwave propagation from changes in plasma-material interactions. Materials studied include aluminum oxide, quartz, and graphite. For each material, global performance metrics of thrust, specific impulse, and total efficiency are measured. Additionally, far-field plasma properties are evaluated using a diagnostic suite consisting of a Langmuir probe, Retarding Potential Analyzer, Faraday probe, and E x B probe. Using these diagnostics, we assess the physical changes to plasma properties that cause differences in global thruster behavior. Armed with these results, we can better understand the effects of back wall material on low-power magnetic nozzle thrusters.

*Work supported by AFOSR Grant FA9550-25-1-0025

References

[1] A. Sheppard and J. Little, JPP. **38,** 6, (2022).
[2] A. Eckhaus and B. Jorns, IEPC. (2025).

Diagnostic Development of X-pinch Backlighters on the MAIZE Pulsed Power Facility *

M. A. Knofczynski [a, b], N. M. Jordan [a] and R. D. McBride[a]

(a) mknofczy@umich.edu University of Michigan, Ann Arbor, MI 48109, USA
(b) Plasma Physics Division, Naval Research Laboratory, Washington, DC 20375

The 1 MA, 8 kJ MAIZE LTD generator at the University of Michigan is a mid-size pulsed power machine capable of simultaneously driving multiple X-pinches. This work presents updates on a planned diagnostic upgrade to improve the temporal and spectral coverage for X-pinch experiments on MAIZE. The diagnostic configuration includes a hybrid X-pinch backlighter setup to create a reliable, time-resolved point source of probing radiation (either soft x-rays or proton beams). X-ray sources can be used for Talbot-Lau x-ray deflectometry or material-dependent monochromatic backlighting, while proton sources enable proton deflectometry measurements and proton radiographic imaging. Promising strategies for improving reliability of the backlighter source include optimized load configurations and adjustable return-current post setups. Additionally, various detector configurations are explored, including gated x-ray cameras, XUV microchannel plate detectors, and scintillator-CCD systems. This proposed platform shows promise to enhance imaging of high density plasmas using hybrid x-pinches to further validate MHD models and support future work in plasma instability growth.

* This work was supported by the DoW SMART Scholarship Program (Sponsoring Facility: Naval Research Laboratory) and by the NNSA's Stewardship Science Academic Alliances Program under DOE Cooperative Agreements DE-NA0004148 and DE-NA0004146.

X-ray Absorption Spectroscopy Measurements of Radiatively Ionized Argon Gas*

K. V. Kelso[a], S. B. Hansen[b], H. J. LeFevre[a], S. R. Klein[a], P. A. Keiter[a,c], R. P. Drake[a] and C. C. Kuranz[a]

(a) University of Michigan, Ann Arbor, Michigan, 48109, USA
(b) Sandia National Laboratories, Albuquerque, New Mexico, 87123, USA
(c) Los Alamos National Laboratory, Los Alamos, New Mexico, 87544, USA

X-ray absorption spectroscopy is a diagnostic tool that can characterize the temperature and ionization state of a plasma. This technique requires experiments to characterize the platform, careful data calibration, and comparison with atomic models to understand the plasma parameters. We performed ionizing radiation wave experiments at the OMEGA Laser Facility that used an ~80 eV X-ray source to heat an Argon (Ar) gas cell at fill pressures of 3 atm. To diagnose the Ar plasma, we used a capsule backlighter offset 10mm from the gas cell, to produce X-rays that were absorbed by the ionized Ar gas. The absorption analysis was calibrated using the significant line structure in the backlighter spectrum, which served as independent energy fiducials enabling definitive measurements of a 50-eV shift in the energy of the Ar K-edge due to ionization. We compare the measured absorption spectra to two independent atomic models, PrismSPECT and SCRAM, and show that the observed K-edge shift in the heated gas is consistent with ionization up to Ar^{+4} and temperatures of 10 eV.

*These experiments were conducted at the Omega Laser Facility with the beam time through the NLUF user program. This work is funded by the DOE-NNSA under cooperative agreement (No. DE-NA0004146 Sandia National Laboratories, under Contract No. DE-NA0003525.

Effects of Elevated Concentrations of Ammonia and Hydrogen Sulfide on Non-Thermal Plasma Inactivation of Airborne Viruses*

Emily M. Hong, Zhenyu Ma and Herek L. Clack

University of Michigan, Civil and Environmental Engineering
(emhong@umich.edu, zhenyuma@umich.edu, hclack@umich.edu)

Airborne viruses are a health concern for both human and livestock health. There has been an increase in outbreaks of avian influenza and other airborne transmissible diseases affecting livestock. To combat the increase in outbreaks, technology suited for inactivating airborne viruses in environmental conditions typical in livestock raising and farming is needed. This study uses non-thermal plasma (NTP) to inactivate airborne viruses in ambient air compositions similar to poultry farm conditions. Ambient air in poultry farms contains high concentrations of ammonia (N) and hydrogen sulfide (H_2S). Poultry farms have varying concentrations of NH_3 and H_2S that exceed 5 ppm [1,2]. Our previous work has established the effects of 1 and 5 ppm of NH_3 and H_2S on NTP inactivation of airborne viruses [3]. This work examines the effects on NTP inactivation of airborne viruses at elevated concentrations of NH_3, 10 and 70 ppm, and H_2S, 10 ppm, using MS2, a bacteriophage considered to act as a conservative surrogate for pathogenic airborne viruses.

Gas cylinders were used for NH_3 trace gas addition [3]. But for more economical and sustainable purposes, we switched to liquid vapor dosing for the elevated concentrations of NH_3. Stable concentrations of NH_3 in flowing air were achieved by exposing compressed air to NH_3 vapors evaporating from 25 mL of liquid household ammonium hydroxide (1-3%) in an open beaker. The open beaker is placed inside an enclosure with a fitting to transport NH_3 into the NTP setup. Trials conducted using this method have achieved an NH_3 concentration level over 10 ppm downstream and have yielded inactivation results comparable to previous results using a gas cylinder. Using the liquid vapor dosing method with 5 mL of 25% ammonium hydroxide will produce dosages between 60-80 ppm of NH_3 comparable to poultry farm conditions.

Previous results for 1 and 5 ppm of NH_3 and H_2S showed statistically significant log inactivation differences with and without trace gases. But between the 1 and 5 ppm of trace gases there was no statistical difference in log inactivation. Our preliminary results are showing 10 ppm of NH_3 log inactivation is not statistically different from 1 and 5 ppm. It is expected that higher concentrations of NH_3 and H_2S will not result in statistically significant differences in log inactivation. A gas cylinder of H_2S will be used to achieve concentrations of 10 ppm H_2S.

*Work supported by the USDA APHIS GC grant.

References

[1] J. Brouček and B. Čermák, Ekologia. **34** (2015)
[2] E. Simsek, et al, CLEAN – Soil, Air, Water. **41** (2013).
[3] Z. Ma, et al., Science of the Total Environment. **939**, 173447 (2024).

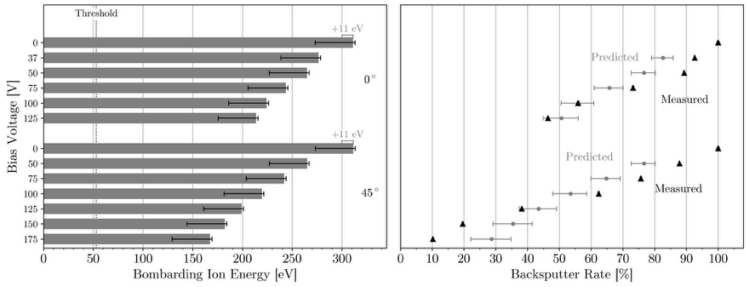
Electrostatic-Magnetic Retardation of a Low-Temperature Ion Beam for Backsputter Mitigation*

Braden Oh, Andrew Schok, Christopher McCullough, Tetiana Tymoshevska and Ben Jorns

U-M Plasmadynamics and Electric Propulsion Laboratory (bradenoh@umich.edu)

Ground-based testing of electric space propulsion (EP) systems, such as Hall effect thrusters (HETs), suffer from facility interaction effects where high-energy exhaust ions sputter material from facility. The resulting backsputtered material deposits back onto the thruster, forming films that severely impede thruster operation and lifetime assessments. While electrostatically retarding ions before impact can drive ion energies below the sputtering threshold, biasing a bare collector plate causes the bulk plasma potential to rise in lockstep with the applied bias due to electron current collection, preventing the establishment of a retarding electric field.

To overcome this limitation, a cusped-field "beam catcher" was designed utilizing permanent magnets behind graphite bias plates to impede electron mobility to the surface. This magnetic impedance enables a localized electrostatic deceleration potential to be established while decoupling the bias voltage from the bulk plasma potential. Experiments were performed at the U-M Large Vacuum Test Facility using a 9-kW-class HET operating on argon propellant. A novel dual Quartz Crystal Microbalance (QCM) diagnostic—combining a standard QCM with a magnetically filtered QCM—was deployed to independently deconvolve neutral carbon deposition from backstreaming ion erosion across bias voltages (0–175 V) and cant angles (0° and 45°)



Filtered QCM measurements demonstrated that carbon backsputter deposition was reduced by 64.1% at a 0° cant (125 V bias) and by 99.5% at a 45° cant (175 V bias). These results confirm that modest reductions in incident ion energy produce disproportionately large decreases in sputter yield due to the nonlinear behavior of sputter yield. Retarding potential analyzer (RPA) traces revealed that higher retarding potentials generate an energetic population of backstreaming ions; however, canting the beam catcher to 45° effectively collimated and steered these ions away from the thruster plane, restoring near-thruster erosion rates to baseline grounded levels. Diagnostic evaluations confirmed that thruster operation was invariant across all beam catcher operating conditions. Magnetically-assisted electrostatic ion retardation thus provides an effective, non-intrusive method for mitigating backsputter in ground testing environments.

*Work supported by NASA through the Joint Advanced Propulsion Institute (JANUS, Grant No. 80NSSC21K1118) and the National Science Foundation Graduate Research Fellowship Program (NSF GRFP).

References

[1] B. Oh, et al., *38th International Electric Propulsion Conference* (2024).
[2] B. Oh, et al., *39th International Electric Propulsion Conference* (2025).

Identifying Informative Designs for Constraining Rheological Properties under Shocked Conditions

Codie Fiedler Kawaguchi[a], Sonya Dick[b], Xun Huan[a] and Eric Johnsen[a]

(a) University of Michigan Mechanical Engineering (cfkawa@umich.edu, xhuan@umich.edu, ejohnsen@umich.edu)

(b) South Dakota School of Mines and Technology, Leslie A. Rose Department of Mechanical Engineering (Sonya.Dick@sdsmt.edu)

Modeling materials with extremely high strain rates such as, shock compression experiments, or materials with extremely low strain rates, such as rheological flows often necessitates modeling solids as a fluid.For example, Earth's mantle, though mostly solid, is treated as a viscous fluid over geological timescales with resistance to flow characterized by an effective viscosity[1][2]. However, experimental constraints on mantle-relevant materials, at appropriate pressures and temperatures remain limited [3][4][5].

Perez et al.[6] tracked the shock-induced Richtmyer–Meshkov (RM) instability growth rate in MgO using one-dimensional velocimetry in experiments fielded at the OMEGA EP Laser Facility. Before the experiment, simulations of the epoxy–MgO interface were performed at different interfacial shock pressures. These simulations were used to examine the perturbation-amplitude evolution and growth rate of the corrugated interface in the linear regime, $a/\lambda < 0.1$.

We extend this work by applying a Bayesian optimal experimental design (OED) framework using a simplified model motivated by the above experiment. Experimental configurations are evaluated using the expected information gain (EIG) to identify experimental conditions that are expected to be most informative for constraining MgO viscosity. The OED framework uses nested Monte Carlo sampling to evaluate the EIG and after data are simulated, posterior inference is performed with Markov Chain Monte Carlo to assess how much the chosen design reduces parameter uncertainty.

References

[1] J. D. Colvin, M. Legrand, B. A. Remington, G. Schurtz, and S. V. Weber. A model for instability growth in accelerated solid metals. Journal of Applied Physics, 93(9):5287–5301, May 2003. ISSN 0021-8979,1089-7550. doi: 10.1063/1.1565188.

[2] K. O. Mikaelian. Effect of viscosity on Rayleigh-Taylor and Richtmyer-Meshkov instabilities. Physical Review E, 47(1):375–383, Jan. 1993. ISSN 1063-651X, 1095-3787. doi:10.1103/PhysRevE.47.375

[3] B. J. Foley. Habitability of Earth-like Stagnant Lid Planets: Climate Evolution and Recovery from SnowballStates. The Astrophysical Journal, 875(1):72, Apr. 2019. ISSN 0004-637X, 1538-4357. doi: 10.3847/1538-4357/ab0f31.

[4] S-i. Karato. Rheological structure of the mantle of a super-Earth: Some insights from mineral physics. Icarus, 212(1):14–23, Mar. 2011. ISSN 00191035. doi: 10.1016/j.icarus.2010.12.005

[5] B. J. Foley, D. Bercovici, and W. Landuyt. The conditions for plate tectonics on super-Earths: Inferences from convection models with damage. Earth and Planetary Science Letters, 331-332:281–290, May 2012.ISSN 0012821X. doi: 10.1016/j.epsl.2012.03.028.

[6] T. M. Perez, S. C. Dick, R. F. Smith, P. M. Celliers, J. H. Eggert, S. J. Ali, E. Johnsen, and J. K. Wicks. Low viscosity of solid MgO at high pressures and strain rates measured using the laser-driven Richtmyer–Meshkov instability. Physical Review B, 111(14), 2025. ISSN 2469-9969. doi: 10.1103/physrevb.111.144108.

Phase-Resolved Optical Emission Spectroscopy of Kr/Water Mixtures in a Pulsed 13.6 MHz RF ICP*

Nicholas Donatelli and Christopher Limbach

University of Michigan, Department of Aerospace Engineering
(donateln@umich.edu, limbach@umich.edu)

In this work, we present the design of a radio-frequency (RF) inductively-coupled plasma source and initial diagnostics using phase-resolved optical emission spectroscopy during pulsed operation. The source design is based on previous work by PPPL and Colorado State University [1,2] and consists of a 4-turn copper coil wrapped outside a 95 mm diameter, 200 mm long quartz discharge tube. The discharge is powered by a 1 kW, 13.56 MHz Advanced Energy Cesar RF generator and Navio Matching network, capable of pulsed operation up to 30 kHz with variable duty cycle.

Optical emission spectroscopy was performed on argon/water mixtures at pressures of 150 mTorr to characterize the steady-state and transient plasma composition. The E-H mode transition was observed at a continuous 285 W accompanied by a spike in atomic H Balmer line, atomic O, and OH A-X emission, as seen in Figure 1 as well as previous work [3].

Preliminary phase-resolved measurements in a N_2 plasma during 10 kHz pulsing at 50% duty cycle show an emission onset time of 30 µs and a decay time of less than 10 µs, highlighted in Figure 2. Future work will investigate how the characteristics of pulsed operation change with gas composition, pressure, and flow rate.

*Work supported by AFOSR and the US Space Force

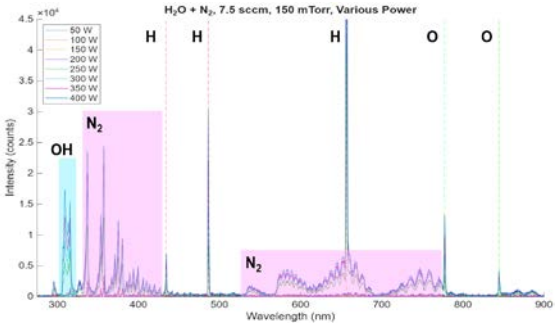


Figure 1 – Preliminary phase resolved OES result highlighting the breakdown, steady-state, and decay of a N_2 plasma at 10 Hz.

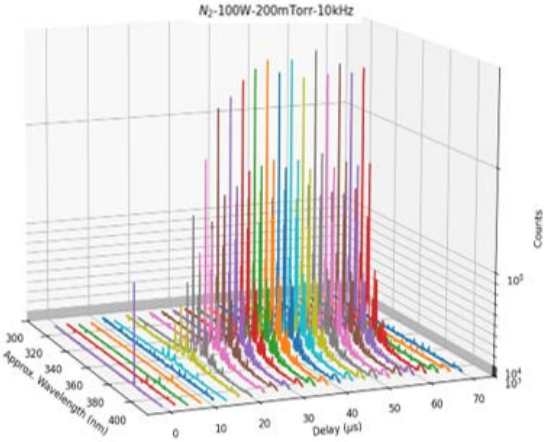


Figure 2 – Preliminary phase resolved OES result highlighting the breakdown, steady-state, and decay stages of a N_2 plasma at 10 Hz.

References

[1] Mitchell C. Morasco, Matteo Da Valle, Seth Thompson and Azer P. Yalin. "Development and Optical Emission Spectroscopy Characterization of a 13.56 MHz RF Plasma Source," AIAA 2026-1227. AIAA SCITECH 2026 Forum. January 2026.

[2] Yevgeny Raitses and Yerbolat Ussenov. "Characterization of Inductively Coupled RF Plasma Source Operating With Molecular Gases for Electric Propulsion," AIAA 2026-2815. AIAA SCITECH 2026 Forum. January 2026.

[3] Su, L., Sheppard, A., Georgin, M., McDonald, M., Experimentally-Measured Species Composition of a Radio-Frequency Cathode Operating with Water, IEPC, 2025.S. Taylor and P. Pix, J. Appl. Phys. **101**, 2389 (2009).

Abstracts: Poster Session III

Comparison of Laser Thomson Scattering and Langmuir Probe Near-Field Electron Measurements on a 9 kW Hall Effect Thruster*

John Riley K. O'Toole and Benjamin A. Jorns

University of Michigan Department of Aerospace Engineering (otoolejr@umich.edu)

Hall effect thrusters (HETs) are currently a leading propulsion technology in-orbit and are a strong candidate to close cis-lunar, Mars, and other deep-space mission architectures. An outstanding challenge for HET design is the interface between theory and experiment; models have to be manually tuned to accurately reproduce measured performance metrics [1]. Traditionally, it is assumed that the peak electron temperature in the acceleration region of HETs scales with the discharge voltage like $0.1Vd$. The evidence for this scaling comes from studies that utilized Langmuir probes to recover axial traces of electron quantities in the near-field plume of these devices [2]. However, the recent development of compact and simple Thomson scattering (TS) diagnostics for low-density plasma sources has offered a non-perturbative glimpse into the near-field electron dynamics that suggests a temperature scaling much closer to 0.20-0.25Vd [3]. Further evidence of this difference measured in this study is shown in Figure 1.

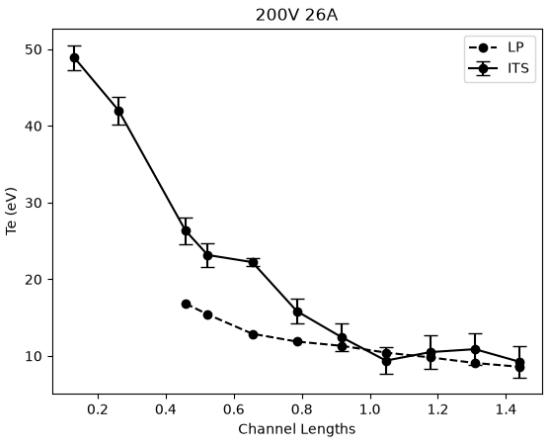


Figure 1 – Comparison of Thomson scattering and Langmuir probe results across a wide axial range in the test articles near-field, operating at 200 V and 26 A.

While studies between these probes have been completed on similar and/or relevant plasma producing devices, to the best of the authors' knowledge, no study has used these techniques in parallel across several thruster conditions to understand these differences. There is therefore an established need to reconcile these two probes in the context of HETs to better aid in matching models to experiment, and to understand the limits of Langmuir probes for studying near-field HET plasma physics.

We will present measurements of electron density and temperature in and around the acceleration region of a 9-kW HET operating on krypton as determined by both TS and Langmuir probes. This analysis will consider the effects of magnetic field, operating conditions, and post-processing techniques to understand why these differences exist and then demonstrate findings for how to reconcile these methodologies.

* Work supported by the NASA Space Technology Graduate Research Opportunities Grant

References

[1] Marks, T. A., and Jorns, B. A., "Modeling anomalous electron transport in Hall thrusters using surrogate methods," 37th International Electric Propulsion Conference, 2022.

[2] Goebel, D. M., and Katz, I., Fundamentals of Electric Propulsion: Ion and Hall Thrusters, JPL Space Science and Technology Series, 2008.

[3] Roberts, P. J., "Characterization of Momentum and Heat Flow in Hall Thrusters with Laser Scattering," Ph.D. thesis, University of Michigan, 2025.

Relativistic Electron Beam Transport and Pulse Broadening in a Diode–Drift System*

Yves Heri and Peng Zhang

University of Michigan, Ann Arbor, MI, USA (heriyves@umich.edu)

Space-charge effects limit current transmission and temporal resolution in ultrafast electron sources. We derive relativistic current limits and a pulse-broadening scaling law for a diode–drift system (Fig. 1), validating the predictions with self-consistent relativistic Lagrangian multiple-sheet simulations [1, 2] and published pulse-width measurements [3].

For a fixed total device length $d = d_g + d_d$, where d_g and d_d are the accelerating-gap and drift lengths, respectively, we define the gap fraction $\xi = d_g/d$ and normalized voltage $U = eV_0/(m_e c^2)$. The steady current-density limit is estimated as

$$J_C = min[J_{RCL}(\xi d, U), J_{RDCL}((1-\xi)d, U)] \quad (1)$$

where J_C is the device limit, and J_{RCL} and J_{RDCL} are the relativistic diode and drift current density limits, respectively. The dimensionless pulse distortion $D = \tau_f/\tau_0$ is

$$D(\xi, U) = \Lambda \frac{1 + (2U+3)\xi^2}{2[U(U+2)]^{3/2}} \quad (2)$$

where $\Lambda = eJd^2/(\varepsilon_0 m_e c^3)$ is the normalized injected current, J is the injected current density. The quantities τ_0 and τ_f denote the initial and detector pulse widths, respectively.

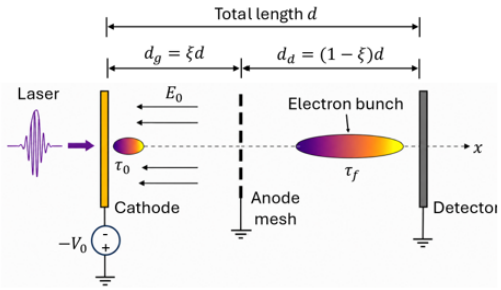


Figure 1. Diode–drift setup with accelerating gap and grounded drift region.

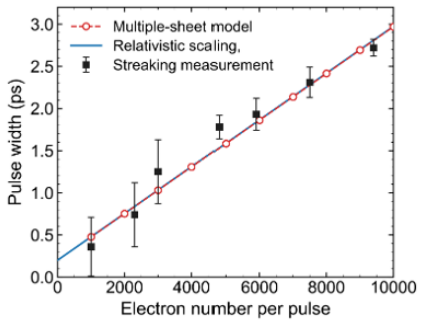


Figure 2. Predicted and measured pulse widths at 60 kV [2].

Steady current peaks where the diode and drift limits coincide, at $\xi = 0.261 \sim 0.306$ for $U = 0.01 \sim 20$. At fixed current density, voltage, and total length, the broadening instead increases with ξ. Thus, maximizing current and minimizing broadening favor different geometries.

At 60 kV, predictions follow measured pulse widths over $10^3 - 10^4$ electrons per pulse (Fig. 2), using a 5 mm gap, 20.5 cm drift, 200 fs initial pulse, and 271 μm beam diameter. The model assumes fixed beam area and neglects initial energy spread.

*This work was supported by the Air Force Office of Scientific Research (AFOSR) Grant Nos. FA 9550-22-1-0523 and FA9550-26-1-B352, and National Science Foundation (NSF) Grant No. 2516752.

References

[1] Y. Heri and P. Zhang, IEEE Trans. Electron Devices 72, 2591–2596 (2025).

[2] Y. Heri, and P. Zhang, IEEE Trans. Electron Devices 73, 3010 (2026).

[3] X. Wang et al., Rev. Sci. Instrum. 80, 013902 (2009).

Extending Plasma Kinetic Theory: Memory, Magnetic Fields, and Strong Coupling*

Jarett LeVan and Scott D. Baalrud

Applied Physics, University of Michigan (jarettl@umich.edu)

Starting from the BBGKY hierarchy, a non-Markovian kinetic equation is derived that extends the validity of the Boltzmann equation to shorter timescales and higher densities, while self-consistently including external fields in the collision operator. The equation is broadly applicable. Its extension to shorter timescales (higher frequencies) enables more accurate modeling of the scattering experiments often used to diagnose plasmas, as well as radiation transport properties and electromagnetic wave absorption. Treatment of the magnetic field within the collision operator enables improved modeling of strongly magnetized plasmas, including trapped antimatter experiments and magnetized inertial confinement fusion (ICF) concepts. And the extension to higher densities enables improved modeling of strongly coupled plasmas, such as those found in astrophysical bodies and produced in ICF implosions. Here, the kinetic equation is applied to predict equilibrium time correlation functions, which characterize the structural and transport properties of fluids. Comparisons with computer simulations and experimental data show that the theory accurately reproduces non-Markovian dynamics in these plasmas.

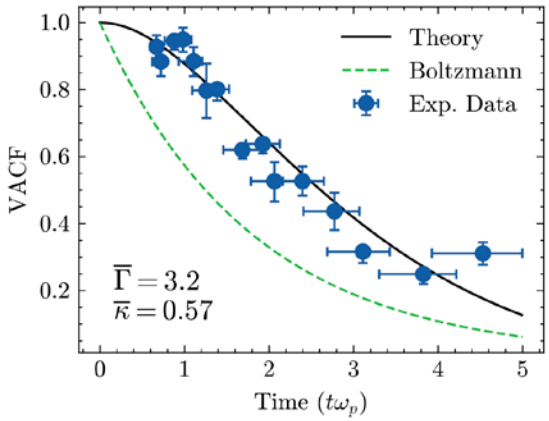


Figure 1 - Normalized velocity autocorrelation function (VACF) in a strongly coupled ultracold neutral plasma. The black solid line is the prediction of the kinetic theory developed in this work, the green dashed line is the Boltzmann equation prediction, and the blue data points are from the experimental measurements of Strickler et al. [1].

*This work was supported by the DOE NNSA Stockpile Stewardship Graduate Fellowship through Cooperative Agreement No. DE-NA0004185, and by award No. DE-NA0004148.

References

[1] Strickler, T. S., Langin, T. K., McQuillen, P., Daligault, J., & Killian, T. C. *Physical Review X*, *6*(2) (2016)

Novel Quasi-Analytic Solutions of Radiation Diffusion in Heterogeneous Media

William Maxon[a], Eric Johnsen[a] and Karthik Duraisamy[b]

(a) Department of Mechanical Engineering, University of Michigan (wmaxon@umich.edu)
(b) Department of Aerospace Engineering, University of Michigan

Accurate numerical modeling of multimaterial fluid systems remains a longstanding challenge, particularly when additional physics, such as radiation transport, are incorporated. In the optically thick limit, where radiation and matter are in local thermodynamic equilibrium and the radiation field is isotropic, the radiation hydrodynamics equations can be reduced to the Euler equations with a modified equation of state when radiation diffusion is negligible. However, conventional finite-volume methods can produce spurious oscillations in pressure and velocity at contact discontinuities, even in the absence of material interfaces. The introduction of multiple materials presents additional challenges for maintaining equilibrium across interfaces. These difficulties motivate the development of robust numerical methods capable of preserving the equilibrium conditions of the underlying physical system. Verification of such methods requires analytical or quasi-analytical reference solutions, which become increasingly difficult to construct as additional physics are incorporated. In this work, two new verification problems for radiation hydrodynamics are presented. The first considers radiation diffusion between two semi-infinite materials with distinct material properties and initially uniform but unequal temperatures, in the absence of material motion. The second considers opaque radiation hydrodynamics, where radiation diffusion is neglected, and develops a quasi-analytical solution to the compressible Riemann problem using a radiation-modified equation of state. These previously unpublished solutions provide reference problems for verifying numerical methods across distinct radiation hydrodynamic regimes, supporting the future development of more accurate and robust numerical simulations.

Quantum-Correct Bhatnagar-Gross-Krook Operator for Coupling Collisions to the Wigner-Poisson Model*

F. Alejandro Padilla Gomez[a], Sining Gong[a], Michael S. Murillo[a], Frank R. Graziani[b], and Andrew Christlieb[a]

(a) Michigan State University (padill77@msu.edu)
(b) Lawrence Livermore National Laboratory

We develop a conservative adaptive-rank method for the periodic 1D1V Wigner–Poisson–BGK system with collisions added through a Fermi–Dirac equilibrium. The principal computational challenge is constructing a nonlinear, moment-dependent equilibrium without assembling the full phase-space distribution. At each collision stage, the chemical potential and thermodynamic temperature are determined from constraints on the incoming local density and kinetic energy. The equilibrium is approximated through sampled entries, and the relaxation update is assembled and compressed directly in low-rank form. A self-consistent correction preserves global mass, momentum, and total energy while accounting for the electric field generated by the corrected distribution [1]. We also examine the moment-feasibility restrictions imposed by the Fermi–Dirac occupation cap, which motivate compatible, quantum-parameter-dependent benchmark families. Numerical experiments consider two-stream, Landau-damping, and bump-on-tail configurations across weakly and strongly collisional regimes. Comparisons with a full-rank method demonstrate decreasing approximation errors as the truncation tolerances are tightened, while the prescribed global invariants are maintained near floating-point precision. Phase-space, electric-energy, and equilibrium diagnostics characterize the distinct relaxation behavior of the benchmark families. The resulting framework integrates Fermi–Dirac relaxation with conservative low-rank quantum transport without a dense BGK update.

*The authors acknowledge support from AFOSR grants FA9550-24-1-0254 and DOE grant DE-SC0023164. AJC is also supported by DOE/NNSA grant DE-NA0004265 and ONR grant N00014-24-1-2242, and the MSU Institute for Cyber-Enabled Research for their computer resources

References

[1] Christlieb, A. J., Gong, S., Qiu, J. M., & Zheng, N. (2026). A Structure-preserving Adaptive-Rank Approach to the High-Dimensional Wigner-Poisson System. *arXiv preprint arXiv:2606.15067*.

Determining Energy Flux Across the Dayside Magnetopause Induced by Boundary Motion*

Nolan Tribu[a], Tuija Pulkkinen[b] and Matti Ala-Lahti[c]

(a) Climate and Space Sciences and Engineering, University of Michigan (ntribu@umich.edu)
(b) Climate and Space Sciences and Engineering, University of Michigan (tuija@umich.edu)
(c) Faculty of Science, University of Helsinki (matti.ala-lahti@helsinki.fi)

We present initial results from quantifying the magnetosphere - magnetosheath energy transfer, along with the main drivers of the energy transport. We especially focus on distinguishing the energy transport associated with boundary motion from the reconnection-driven transport across the boundary. Global magnetohydrodynamic (MHD) simulations have demonstrated the large-scale locations of the energy flow across the boundary and its relation to both magnetic reconnection and boundary motion[1]. We have carried out a comprehensive investigation of the energy flux across the low-latitude dayside magnetopause that is based on high-resolution in-situ observations from Magnetospheric Multiscale (MMS) mission during over 4000 well defined magnetopause crossings. Initial statistical results agree with simulations in cases where the crossings are across well defined Harris sheet-like boundaries, with the general direction of the flux is energy leaving the magnetosphere to the magnetosheath[2]. The dominant energy flux transport is connected to the boundary motion, which results in the interior energy flux within the boundary layer to lack correlation with the upstream solar wind. On the other hand, the net flux into or out of the boundary layer itself is connected to local scale interactions at the magnetopause.

*Work Supported by NSF Grant No. 2420675. MA-L and TP also acknowledge the NSF Grant No. 2033563 and NASA Federal Award No. 80NSSC23M0192.

References

[1] Brenner, A., Pulkkinen, T. I., Al Shidi, Q., and Toth, G. (2021), Storm-time Energetics: Energy Transport Across the Magnetopause in a Global MHD Simulation. Front. Astron. Space Sci. 8, 180

[2] Paschmann, G., Haaland, S. E., Phan, T. D., Sonnerup, B. U. Ã., Burch, J. L., Torbert, R. B., Gershman, D. J., Dorelli, J. C., Giles, B. L., Pollock, C., Saito, Y., Lavraud, B., Russell, C. T., Strangeway, R. J., Baumjohann, W., and Fuselier, S. A.: Large-Scale Survey of the Structure of the Dayside Magnetopause by MMS, J. Geophys. Res.-Space, 123, 2018–2033, 2018.

Development and Characterization of an Al Vapor Target for Ionization Front Experiments*

N. S. Bowers[a,b], A. Uras[b], L. G. Suttle[b], E. Kriz[b], A. P. Button[b], S. Merlini[b], J. Stručka[2], T. R. Mundy[b], K. Marrow[b], S. N. Bland[b], S. V. Lebedev[b]

(a) Applied Physics Program, The University of Michigan, Ann Arbor, USA (nsbowers@umich.edu)
(b) Blackett Laboratory, Imperial College London, London, United Kingdom

We present initial data on the development and characterization of a low-density, Aluminum vapor column target for use in ionization front experiments at the MAGPIE pulsed-power facility at Imperial College London. Spatially resolved interferometry (532nm and 355nm), optical self-emission, and electronic diagnostics were used to diagnose the target. The target was neutral, highly uniform on axis with peak densities of $n \approx 10^{19}\mathrm{cm}^{-3}$ and an effective initial speed of sound of 1.4km/s. Initial results indicate a supersonic ionization wave was able to be driven through the target which reached ionization fractions above 80%.

*This research is supported by the EPSRC and First Light Fusion under the AMPLIFI Prosperity Partnership EP/X025373/1; AFOSR under FA8655-23-1-7062; Sandia National Laboratories; and the NNSA under DOE DE-NA0004148.

DMSP SSUSI & SSJ Auroral Oval Model Validation

Michelle X. Bui, Sreelakshmi Jayaraman, Daniel Welling, Tuija Pulkkinen,

Chen Wu and Aaron Bukowski

University of Michigan, Department of Climate and Space Science and Engineering (mxbui@umich.edu)

Earth's aurora is generated by energetic precipitation into our ionosphere at the polar regions. Auroras are observable in a region known as the auroral oval, which is affected by Earth's magnetic field and its interaction with the solar wind. During major space weather events, solar wind-magnetosphere interaction can alter the auroral oval morphology and intensity, changing the energy deposition into the polar ionosphere. The auroral oval energy flux can be observed by DMSP-SSUSI, the Special Sensor Ultraviolet Spectrographic Imager aboard the Defense Meteorological Satellite Program, while the low energy particle precipitation can be measured by DMSP-SSJ, the Special Sensor J for Precipitating Ion and Electron Spectrometer. SSUSI scans a partial swath of the auroral oval, and along the same path, SSJ scans the energy spectrum for particle fluxes between 30 eV to 30 KeV. These observations can be compared with auroral models that are being developed not only to resolve limited observational capacities but also to achieve predictive capabilities. Auroral models can fill observational gaps, but their performance is not well quantified.

We are developing a toolkit to access case-study comparisons between auroral observations and model predictions as well as statistics over multiple storms. The toolkit tracks the geoeffectiveness of the storm event, calculates metrics to determine the differences between observed and modeled auroral oval response, and compares these metrics across a range of storms. We define metrics of the auroral oval response using both the intensity of energy input and the auroral morphology. The intensity can be quantified as the integrated hemispheric power, the total energy flux over the auroral oval area. The morphology can be traced by the auroral oval boundaries, from the boundary between closed and open magnetic field lines to the equatorward boundary, tracking the extent to which the auroral oval expands in response to the storm. We employ a k-means clustering algorithm to identify the boundaries at a given threshold. We are testing this toolkit for several empirical and physical auroral models, including OVATION, FTA, and SWMF Geospace with CMEE. In this presentation, we show initial comparisons to characterize model performance and describe our next steps to quantitative validation.

Calculating the Thermal Conductivity of a Two-Component Plasma Using Non-equilibrium Molecular Dynamics Simulations*

Briggs Damman[a], Jarett LeVan[a] and Scott Baalrud[b]

(a) Applied Physics Department, University of Michigan
(b) Nuclear Engineering and Radiological Sciences Department, University of Michigan

Non-equilibrium molecular dynamics (MD) simulations are run with the goal of calculating the total thermal conductivity spanning weak to strong Coulomb coupling. Transport coefficients, such as the thermal conductivity, are used to connect gradients in thermodynamic variables to fluxes, and previous works have computed these transport coefficients from equilibrium MD simulations using the Green-Kubo formalism [1]. However, only the kinetic portion of the transport coefficients were able to be evaluated due to divergences in both the potential and virial components. It is expected that these potential and virial components are the dominant contributor to the transport coefficients at strong coupling. In this work, the temperature decay rate calculated from non-equilibrium MD is found to converge at any coupling strength and is related to the thermal conductivity. Further, the Green-Kubo relations are revisited to find the source of the divergences and reinterpreted to be consistent with the non-equilibrium results.

*This material is based upon work supported by NSF Grant Award No. PHY-2512424

References

[1] Damman B, LeVan J, Baalrud S. D. "Molecular Dynamics Simulation of Hydrodynamic Transport Coefficients in Plasmas." *Phys. Plasmas* 33, 032117 (2026).

Platform for X-Pinch Radiography Capability of Shock Propagation Through a Foam

Filomela V. Gerou, Adam Bedel, Nick Jordan and Ryan D. McBride

Nuclear Engineering and Radiological Sciences, University of Michigan, Ann Arbor, MI, USA
(fgerou@umich.edu)

We present a computational framework for studying shock propagation via radiography using an X-pinch platform at the MAIZE pulsed-power facility.[1] We develop this novel platform to study shock wave propagation via X-pinch exploding wires within foam at MAIZE. Although X-pinch shock geometries have been demonstrated at large installations, compact pulsed-power drivers remain comparatively underexplored for producing planar shock systems within foam. The initial experimental configuration proposed employs two exploding wires that launch shocks into a central CH foam [1] generating an X-ray drive diagnosed through time-resolved X-ray imaging. Specifically, the geometry represents a pair of X-Pinches representing the shock driver and radiography back-lighter. We computationally explore various exploding wire and fast imaging configurations. We report on project status in platform development and in studying radiation transport through foam. We develop and benchmark a FLASH two-dimensional resistive magnetohydrodynamic model tailored to MAIZE operating conditions. The model may be used in establishing scaling relations that connect our laboratory pulsed-power shock propagation via a medium to astrophysical accretion disk shocks. This platform enables controlled investigations of shock formation and provides a compact-facility analogue for X-pinch shock processes through foam.

References

[1] G. V. Dowhan, A. P. Shah, B. J. Sporer, N. M. Jordan, S. N. Bland, S. V. Lebedev, R. A. Smith, L. Suttle, S. A. Pikuz, R. D. McBride; High-magnification Faraday rotation imaging and analysis of X-pinch implosion dynamics. *Rev. Sci. Instrum.* 1 April 2024; 95 (4): 043504. https://doi.org/10.1063/5.0178321

Tailored Voltage Waveforms in Inductively Coupled Plasmas for Cryogenic Etching using Ar/HF Gas Mixtures*

Yifan Gui[a], Yeon Geun Yook[a], Chenyao Huang[a], Saravanapriyan Sriraman[b] and Mark J. Kushner[a]

(a) University of Michigan, 1301 Beal Avenue, Ann Arbor, MI 48109-2122, USA
(evangyf@umich.edu, ygyook@umich.edu, chenyaoh@umich.edu, mjkush@umich.edu)
(b) Lam Research Corporation, 4305 Cushing Pkwy., Fremont, CA 94538, USA
(Saravanapriyan.Sriraman@lamresearch.com)

In microfabrication, fabricating high aspect ratio (HAR) dielectric features has relied on capacitively coupled plasma (CCP) reactors using fluorocarbon chemistries. In these systems, process parameters are tuned to optimize the production of C_xF_y fragments and ion energy distributions with the end goal of balancing polymer deposition and chemical sputtering to maintain profile control and etch rate. Inductively coupled plasmas (ICPs) have not been extensively used for dielectric etching due to the difficulty in controlling the fragmentation of the fluorocarbon gases. Cryogenic plasma etching of dielectrics typically uses HF based chemistries which relies on water-HF condensation and physisorption rather than the thickness and composition of the fluorocarbon polymer passivation layer. Consequently, the need to optimize of C_xF_y dissociation is eliminated, which then makes ICPs more attractive for cryogenic etching system. Decoupling plasma generation by the source power and ion acceleration by the bias power is also less difficult using ICPs.

In this presentation we discuss results from a computationally investigation of the use of voltage waveform tailoring (VWT), specifically a rectangular bias (RB) waveform, in ICPs for cryogenic etching of dielectrics. RB waveforms generate a more mono-energetic ion energy distribution to the substrate compared to sinusoidal biases. This investigation was performed using, the Hybrid Plasma Equipment Model (HPEM), a modular simulator designed for low-pressure plasma systems. This study focuses on the evolution of incident fluxes and energy angular distributions (EADs) for electrons and ions onto wafers for ICPs operating at pressures of tens of mTorr with Ar/HF feed gas. We will discuss the impact of an expanded operational space (plasma source type, power/voltage scaling, and waveform) on the resulting EADs and flux uniformity across the wafer.

*Work supported by Lam Research, Samsung Electronics and Department of Energy Office of Fusion Energy Sciences.

Effect of Temporal Optical Pulse Asymmetry on Ultrafast Photoemission*

Lan Jin and Peng Zhang

Department of Nuclear Engineering and Radiological Sciences, University of Michigan, Ann Arbor, Michigan 48109, USA (umpeng@umich.edu)

Ultrafast photoemission is governed not only by pulse energy and peak field, but also by the temporal and spectral waveform of the driving optical field. For few-cycle pulses and nonlinear photoemission conditions, the emitted-electron yield and spectrum can be sensitive to the instantaneous field, carrier-envelope phase (CEP), pulse duration, and spectral bandwidth [1–3]. Most theoretical studies nevertheless assume temporally symmetric optical pulse envelopes. In experiments, however, femtosecond pulses can develop unequal leading and trailing edges because of residual spectral phase, incomplete compression, nonlinear propagation, and limitations of practical pulse-shaping systems [4, 5]. Temporally asymmetric pulses can also be deliberately generated by tuning grating compressors [5]. Previous calculations further show that the temporal pulse profile can significantly affect photoemission, particularly at low intensities where emission is sensitive to the high-energy tail of the optical spectrum [6]. These observations motivate the study of temporal pulse asymmetry in ultrafast photoemission.

In this work, we investigate how temporal asymmetry influences ultrafast photoemission using a bi-Gaussian pulse with independently adjustable rise and fall durations. We define a temporal asymmetry parameter $s = \frac{\tau_f}{\tau_r}$, where τ_r and τ_f are the rise and fall durations of the bi-Gaussian pulse, respectively. A value of $s = 1$ represents a symmetric pulse, $s < 1$ corresponds to a slower rise and faster fall, and $s > 1$ correspond to a faster rise and slower fall. Using an exact quantum photoemission framework [7], we investigate how temporal pulse asymmetry influences ultrafast photoemission under a range of optical conditions. The study aims to determine how strongly photoemission depends on unequal rise and fall times, how this sensitivity evolves with field strength, and whether temporal asymmetry can serve as an additional degree of freedom for tailoring ultrafast electron emission. More broadly, the results will help establish when the commonly assumed symmetric pulse envelope is sufficient and when realistic pulse asymmetry should be included in quantitative theory-experiment comparisons.

*This work was supported by the Air Force Office of Scientific Research (AFOSR) Grant Nos. FA 9550-22-1-0523 and FA9550-26-1-B352, and National Science Foundation (NSF) Grant No. 2516752.

References

[1] M. Krüger, M. Schenk, and P. Hommelhoff, Nature 475, 78–81 (2011).
[2] B. Piglosiewicz, S. Schmidt, D. J. Park, J. Vogelsang, P. Groß, C. Manzoni, P. Farinello, G. Cerullo, and C. Lienau, Nat. Photonics 8, 37–42 (2014).
[3] L. Jin and P. Zhang, Phys. Rev. Research 8, 013035 (2026).
[4] M. Guesmi, P. Veselá, and K. Žídek, Sci. Rep. 12, 3827 (2022).
[5] C. Tóth, J. Faure, J. van Tilborg, C. G. R. Geddes, C. B. Schroeder, E. Esarey, and W. P. Leemans, Opt. Lett. **28**, 1823–1825 (2003).
[6] H. Jouin and G. Duchateau, Phys. Rev. A 99, 013433 (2019).
[7] Y. Luo, Y. Zhou, and P. Zhang, Phys. Rev. B 103, 085410 (2021).

Spatial Anti-aliasing Optical Plasma Wave Diagnostics for Low Temperature Plasma Sources

Miron Liu and Benjamin Jorns

Department of Aerospace Engineering, University of Michigan

Measuring high-frequency, small length-scale plasma waves in low temperature plasma sources has been a long-standing and unresolved challenge. These waves are believed to facilitate the anomalous transport of particles and energy in these devices, manifesting as reduced device performance and accelerated device erosion [1, 2]. Given the apparent deleterious influence of these modes on electron and ion dynamics, there has been a concerted effort to incorporate their effects into models of electric propulsion plasmas. Unfortunately, limitations in current plasma wave diagnostics have precluded direct experimental measurements of fundamental wave properties, which are key to achieving a comprehensive understanding of these modes, and in turn, their exact relationship to anomalous transport phenomena. The principle limitations of plasma wave diagnostics lie in the limited spatial bandwidths of physical probes, as well as the perturbative nature of these probes. There is thus an apparent need to develop higher-bandwidth, non-perturbative plasma wave diagnostics. The goal of this work is to address this need. To this end, we present in this work a method based on spatial anti-aliasing which increases the bandwidth of probe-based plasma wave diagnostics by an order of magnitude. We also present preliminary work on adapting conventional laser induced fluorescence velocimetry systems for non-perturbative detection of high-frequency, small length scale plasma waves in low temperature plasma sources.

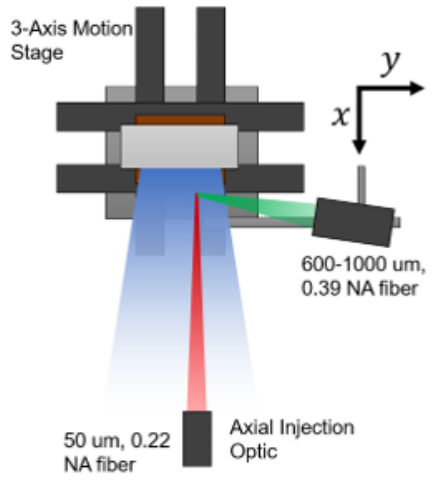


Figure 1 - Conventional Laser Induced Fluorescence (LIF) for Ion Velocimetry

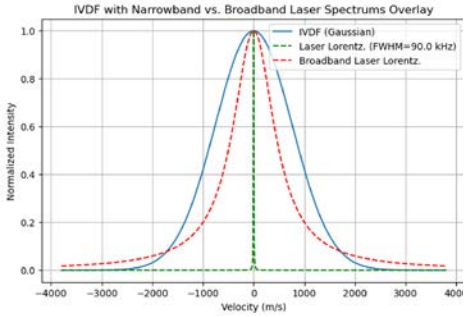


Figure 2 - Spectral Spreading Scheme to Increase Signal-to-Noise

*Work supported by NASA Space Technology Graduate Research Opportunity (NSTGRO) and Rackham Merit Fellowship (RMF)

References

[1] J. D. Frieman, H. K. Kamhawi, P. Y. Peterson, D. A. Herman, J. H. Gilland, R. R. Hofer, AIAA P&E Forum, (2019).

[2] Sengupta, A., Brophy, J. R., Anderson, J. R., Garner, C. E., de Groh, K. K., and Karniotis, T., "An Overview of the Results from the 30,000 Hr Life Test of Deep Space 1 Flight Spare Ion Engine," 40th AIAA/ASME/SAE/ASEE Joint Propulsion Conference and Exhibit, 2004. https://doi.org/10.2514/6.2004-3608.

High-energy Narrow-divergence Electron Beam Generation from High Intensity Solid Target Interactions Using the ZEUS Laser System*

Jeremy Rebenstock, Veronica Contreras, Paul Campbell, Yong Ma, Milos Burger, Che-Hao Chang, Matthew Shepherd, Mirielle Wong, Qian Qian, Anatoly Maksimchuk, John Nees, Louise Willingale and Karl Krushelnick

Center for Ultrafast Optical Science, University of Michigan

Measurements of energetic electron beams from 2 PW laser interactions with solid targets are presented. The experiments were conducted using the Zettawatt Equivalent Ultrashort pulsed laser System (ZEUS) at the University of Michigan with a very long focal length (f/70) focusing geometry and a peak intensity of about 10^19 W/cm^2. We report narrow divergence electron beams (theta ~ 30 mrad) which were measured from the front surface of the target in the near specular direction. Along with the electron beam, highly directional low order harmonic emission including 5/2w and 4/3w were also simultaneously measured in the specular direction

*Work supported by the National Science Foundation.

Intrinsic Mean Transverse Energy in Electron Emission Across Multiple Emission Regimes*

Tianqi Sun[a] and Peng Zhang[b]

(a) Department of Materials Science and Engineering, University of Michigan, Ann Arbor, Michigan 48109, USA (tianqis@umich.edu)
(b) Department of Nuclear Engineering and Radiological Sciences, University of Michigan, Ann Arbor, Michigan 48109, USA (umpeng@umich.edu)

Electron beams with high brightness and low mean transverse energy (MTE) are crucial in particle accelerators, radiation sources, and plasma sciences. They enable applications such as free electron lasers, ultrafast electron microscopy, and high power microwaves and light sources.[1,2] While existing theories can predict MTE in the linear photon absorption range or in the above-threshold emission regime, they are not applicable in strong-field regimes and cannot reliably predict MTE across the full range of emission mechanisms.[3]

This work presents a unified theory for predicting MTE of emitted electrons from photocathodes across multiple emission regimes, including thermionic, DC field, single-photon over-the-barrier, multiphoton absorption emission, and strong-field emission. We present a methodology to calculate electron emission probabilities and MTE by exactly solving the time-dependent Schrödinger equation (TDSE) with arbitrary combinations of DC and laser fields.[4]

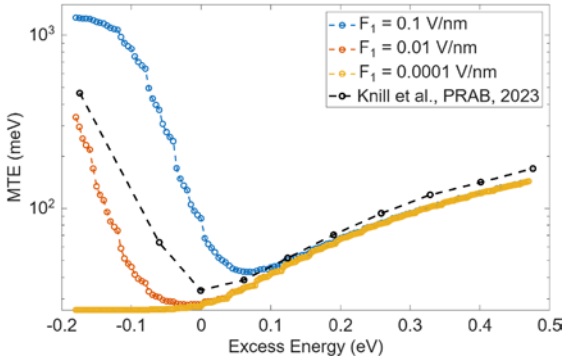


Figure 1 – Comparison between experimentally measured MTEs in two different emission regimes (single photon absorption and multiphoton absorption regimes) and theoretically predicted values using the developed theory.

This unified model reproduces experimentally measured MTE values in the single-photon absorption and thermionic emission regimes at arbitrary temperatures.[5] It also enables accurate MTE predictions in non-linear photoemission regimes such as multiphoton absorption.[6] The model can serve as a theoretical guide for determining the intrinsic MTE across various electron emission regimes.

*This work was supported in part by the Air Force Office of Scientific Research (AFOSR) under Grant FA9550-22-1-0523, in part by the Air Force Office of Scientific Research (AFOSR) under Grant FA9550-26-1-B352, and in part by the National Science Foundation (NSF) under Grant 2516752.

References

[1] A. F. Habib et al., Nat Commun **14**, 1054 (2023).
[2] J. Benford, E. Schamiloglu, J. C. Stephens, J. A. Swegle, and P. Zhang, *High Power Microwaves*, 4th Edition (CRC Press, Abingdon, Oxon; Boca Raton, FL, 2025).
[3] D. H. Dowell and J. F. Schmerge, Phys. Rev. ST Accel. Beams **12**, 074201 (2009).
[4] P. Zhang and Y. Y. Lau, Scientific Reports **6**, 19894 (2016).
[5] A. Kachwala et al., Applied Physics Letters **123**, 044106 (2023).
[6] C. J. Knill et al., Phys. Rev. Accel. Beams **26**, 093401 (2023).

Conceptual Design of an Electrospray-Enabled Liquid Droplet Radiator*

Tetiana Tymoshevska and Benjamin Jorns

Department of Aerospace Engineering at the University of Michigan (tanyaty@umich.edu)

As the power required for future space exploration missions enabled by nuclear electric propulsion increases, there will be a growing need for efficient methods of heat rejection. Current proposed thermal management systems for space reactors require enormous area, representing a dominant driver of the specific mass (kg/kW) for the system [1]. The Liquid Droplet Radiator (LDR) is in principle an attractive low specific mass alternative because they radiate heat out into space through millions of individual tiny droplets. One of the chief limitations preventing their adoption has been the challenge of how to generate the droplets in the LDR with sufficient uniformity and collimation. To overcome this problem, this effort explores a novel approach: the use of electrosprays—a highly tunable and versatile method for droplet generation---to produce the droplet sheets.

Electrosprays are a form of droplet generation commonly employed in mass spectrometry and in some electric propulsion systems that operate on the principle of applying a large voltage difference between an emitter and extractor grid to eject a conducting liquid stream. The charged nature of the droplets offers in principle a high degree of control for sheet formation and speed—both critical factors for efficient LDRs. With that said, LDRs have a unique set of requirements not typically considered in current electrospray literature: a high volumetric flow rate of large, slow-moving droplets and a conducting liquid that is stable at high temperatures [2].

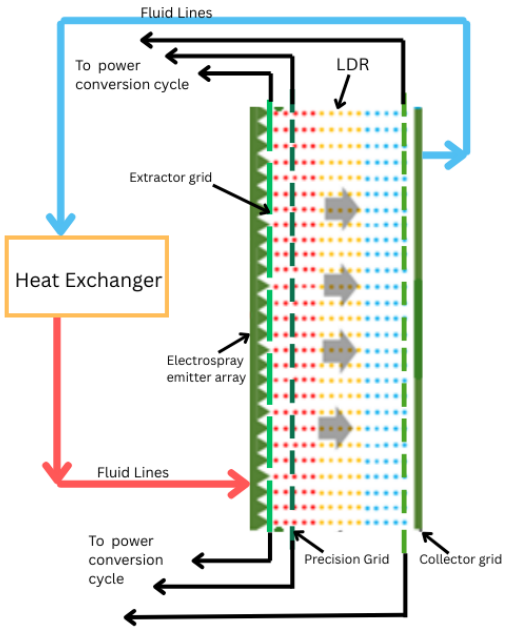


Figure 1 – Electrospray enabled Liquid Droplet Radiator concept of operations.

The current work overviews the concept of operations of the LDR with electrosprays. The relevant scaling laws for droplets are presented as well as the scaling laws for electrospray-driven droplet formation [3]. These governing relations are balanced to present a preliminary design for an electrospray geometry and LDR configuration capable of rejecting up to 1 kW of power at 200 C rejection temperature.

*Work supported by NASA Space Technology Graduate Research Opportunity (NSTGRO)

References

[1] Chong, D., Zhu, M., Zhao, Q. et al. “A Review on Thermal Design of Liquid Droplet Radiator System”. J. Therm. Sci. 30, 394–417 (2021)

[2] A. T. Mattick and A. Hertzberg, “The Liquid Droplet Radiator—an Ultralightweight Heat Rejection System for Efficient Energy Conversion in Space,” *Acta Astronautica*, vol. 9, 165–172 (1982)

[3] A. M. Gañán-Calvo, J. Dávila, and A. Barrero, “Current and Droplet Size in the Electrospraying of Liquids. Scaling Laws,” *Journal of Aerosol Science*, vol. 28, no. 2, 249–275 (1997)

Coherent Spectroscopy of Rydberg Levels in Discharge Plasma for Electric Field Sensing

Xinyan Xiang[a], Bineet Dash[a], Dingkun Feng[a], Eric Paradis[b] and Georg Raithel[a]

(a) University of Michigan Ann Arbor (xinyann@umich.edu)
(b) Eastern Michigan University (eparadis@emich.edu)

We present a non-invasive spectroscopic technique to measure electric fields in a continuous discharge plasma, leveraging large polarizabilities and Stark shifts of Rydberg levels. The Stark shifts are measured via Electromagnetically Induced Transparency (EIT) of Rb vapor seeded into the continuous, inductively coupled radio-frequency (rf) plasma in tens of mTorr of Ar gas. Without plasma, the Rydberg-EIT spectra exhibit rf modulation sidebands caused by electric- and magnetic-dipole transitions induced by the rf drive coil. With the plasma present, the rf sidebands are suppressed, in part due to rf screening. The line shapes in the bulk of plasma reflect the ions' Holtsmark microfield distribution and collisional line broadening. The spectra allow us to determine the plasma density over a range of pressures and rf drive powers. The work has applications in non-invasive spatio-temporal electric-field diagnostics in low-pressure plasma, plasma sheaths, and dusty plasma.

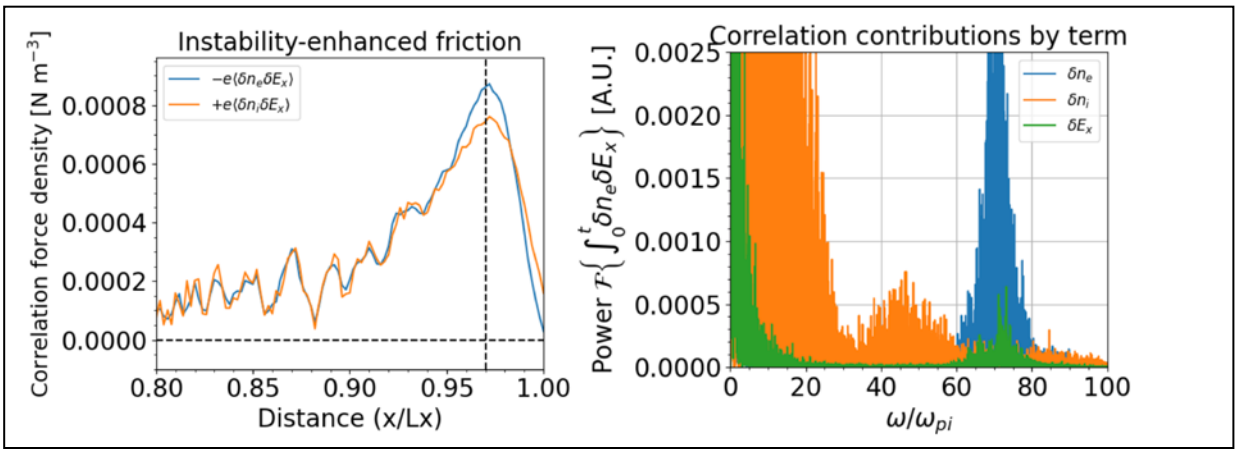
Kinetic-informed Fluid Model for Cross-field Sheaths in Multi-ion Species Plasmas*

Moises Angulo Enriquez and Scott Baalrud

Department of Nuclear Engineering and Radiological Sciences, University of Michigan
(moisesae@umich.edu)

Cross-field sheaths form when magnetic fields are applied parallel to an absorbing wall, causing the plasma loss rate to depend on diffusion across magnetic field lines. Previous work has shown that electron-neutral scattering can provide a mechanism to support classical sheath formation in sufficiently collisional regimes [1]. However, at low pressures this collisional transport description is expected to break down in partially magnetized plasmas. Here we present new PIC-MCC results suggesting a transition between neutral-scattering-dominated transport and anomalous transport driven by wave-particle scattering from kinetic instabilities. Magnetic-field and neutral-density scans show that the electron cross-field diffusion can exceed the classical electron-neutral rate by orders of magnitude. Spectral analysis identifies several fluctuation branches, including electron Bernstein modes and a coupled ECDI/ion-acoustic-like mode that may provide the dominant scattering mechanism [2]. To connect this instability to reduced modeling, we use an ion-trapping saturation model to estimate the nonlinear fluctuation amplitude and infer an effective scattering rate [3]. This rate is then used to close a drift-diffusion model, which is coupled to a near-wall kinetic loss-orbit description to predict modified sheath formation in cross-field geometries.

*This research is supported by the U.S. Department of Energy Isotope Program, managed by the Office of Science for Isotope R&D and Production.



References:

[1] Moritz, J., et al. "The plasma-wall transition layers in the presence of collisions with a magnetic field parallel to the wall." Physics of Plasmas 25.1 (2018).

[2] Hara, Kentaro, and Sedina Tsikata. "Cross-field electron diffusion due to the coupling of drift-driven microinstabilities." Physical Review E 102.2 (2020): 023202.

[3] Lafleur, Trevor, S. D. Baalrud, and Pascal Chabert. "Theory for the anomalous electron transport in Hall effect thrusters. II. Kinetic model." Physics of Plasmas 23.5 (2016): 053503.

List of Participants

First name	Last name	Email	University
Lucas	Babati	lbabati@umich.edu	U-M
Katie	Ballard	bllrdk@umich.edu	U-M
Nathaniel	Bowers	nsbowers@umich.edu	U-M
Declan	Brick	brickd@umich.edu	U-M
Adam	Brusstar	anbruss@umich.edu	U-M
Michelle	Bui	mxbui@umich.edu	U-M
Gonçalo	Cardoso	gcardoso@umich.edu	U-M
Victoria	Collemi	vcollemi@umich.edu	U-M
Briggs	Damman	bdamman@umich.edu	U-M
Jesus	Diaz Alcala	diazalc@umich.edu	U-M
Nicholas	Donatelli	donateln@umich.edu	U-M
Ari	Eckhaus	aeckhaus@umich.edu	U-M
Moises	Enriquez	moisesae@umich.edu	U-M
Md Arifuzzaman	Faisal	faisalmd@umich.edu	U-M
Sarah	Feldman	sarfeldm@umich.edu	U-M
Codie	Fiedler Kawaguchi	cfkawa@umich.edu	U-M
Ian	Freeman	freem386@msu.edu	MSU
Josh	Fung	joshfung@umich.edu	U-M
Filomela V.	Gerou	fgerou@umich.edu	U-M
Myles	Gong	mygong@umich.edu	U-M
Corey	Gui	coreygui@umich.edu	U-M
Yifan	Gui	evangyf@umich.edu	U-M
Jiashu	Han	shujhan@umich.edu	U-M
Yves	Heri	heriyves@umich.edu	U-M
Emily	Hong	emhong@umich.edu	U-M
Chenyao	Huang	chenyaoh@umich.edu	U-M

First name	Last name	Email	University
Jisu	Jeon	jisujeon@umich.edu	U-M
Lan	Jin	jinlan@umich.edu	U-M
Ishan	Kanade	ikanade@umich.edu	U-M
Shane	Keiser	sakeiser@umich.edu	U-M
Kwyntero	Kelso	kkelso@umich.edu	U-M
Kyle	Kemmerer	kylekem@umich.edu	U-M
Julian	Kinney	julkin@umich.edu	U-M
Marissa	Knofczynski	mknofczy@umich.edu	U-M
Carter	Krumins	ckrumins@umich.edu	U-M
Jarett	LeVan	jarettl@umich.edu	U-M
Miron	Liu	mironliu@umich.edu	U-M
Alexander	Loomis	loomisa6@msu.edu	MSU
William	Maxon	wmaxon@umich.edu	U-M
Braden	Oh	bradenoh@umich.edu	U-M
John Riley	O'Toole	otoolejr@umich.edu	U-M
Alejandro	Padilla Gomez	padill77@msu.edu	MSU
Jeremy	Rebenstock	jrebenst@umich.edu	U-M
Adam	Rouzky	arouzky@Umich.edu	U-M
Wanglim	Song	wlsong@umich.edu	U-M
Tianqi	Sun	tianqis@umich.edu	U-M
Alex	Timoney	timoney@umich.edu	U-M
Nolan	Tribu	ntribu@umich.edu	U-M
Tetiana	Tymoshevska	tanyaty@umich.edu	U-M
Bingqing	Wang	bqwang@umich.edu	U-M
James	Welch	welchjc@umich.edu	U-M
Xinyan	Xiang	xinyann@umich.edu	U-M
Yeon Geun	Yook	ygyook@umich.edu	U-M
Grace	Zoppi	gzoppi@umich.edu	U-M